An active back-support exoskeleton to reduce spinal loads: actuation and control strategies

DISSERTATION

Stefano TOXIRI

Department of Advanced Robotics
Istituto Italiano di Tecnologia
and
Dipartimento di Informatica, Bioingegneria, Robotica e Ingegneria dei Sistemi
Università degli Studi di Genova

Supervisors:
Dr. Jesús ORTIZ
Prof. Darwin G. CALDWELL

External reviewers:
Dr. Simona CREA
Prof. Konrad S. STADLER

January 19, 2018

Abstract

Wearable exoskeletons promise to make an impact on many people by substituting or complementing human capabilities. There has been increasing interest in using these devices to reduce the physical loads and the risk of musculoskeletal disorders for industrial workers. The interest is reflected by a rapidly expanding landscape of research prototypes as well as commercially available solutions. The potential of active exoskeletons to reduce the physical loads is considered to be greater compared to passive ones, but their present use and diffusion is still limited.

This thesis aims at exploring and addressing two key technological challenges to advance the development of active exoskeletons, namely actuators and control strategies, with focus on their adoption outside laboratory settings and in real-life applications. The research work is specifically applied to a back-support exoskeleton designed to assist repeated manual handling of heavy objects. However, an attempt is made to generalise the findings to a broader range of applications.

Actuators are the defining component of active exoskeletons. The greater the required forces and performance, the heavier and more expensive actuators become. The design rationale for a parallel-elastic actuator (PEA) is proposed to make better use of the motor operating range in the target

task, characterized by asymmetrical torque requirements (i.e. large static loads). This leads to improved dynamic performance as captured by the proposed simplified model and measures, which are associated to user comfort and are thus considered to promote user acceptance in the workplace.

The superior versatility of active exoskeletons lies in their potential to adapt to varying task conditions and to implement different assistive strategies for different tasks. In this respect, an open challenge is represented by the compromise between minimally obtrusive, cost-effective hardware interfaces and extracting meaningful information on user intent resulting in intuitive use. This thesis attempts to exploit the versatility of the active back-support exoskeleton by exploring the implementation of different assistive strategies. The strategies use combinations of user posture and muscular activity to modulate the forces generated by the exoskeleton.

The adoption of exoskeletons in the workplace is encouraged first of all by evidence of their physical effectiveness. The thesis thus complements the core contributions with a description of the methods for the biomechanical validation. The preliminary findings are in line with previous literature on comparable devices and encourage further work on the technical development as well as on more accurate and specific validation.

ACKNOWLEDGMENTS

The three years leading to this thesis have been a life-changing experience. If I have managed to turn the challenges into achievements and growth, it is thanks to the people that have been part of my life. I am truly grateful for their presence and humbled by their example. In some ways, I consider them "co-authors" of this achievement.

Jesús has been a quiet model, *the* example of leading by example, with his rare patience, perserverance and genuine trust. The connection with Andrea started as a coincidence and has evolved into a fruitful collaboration. His calmness and keen dedication have been of stimulating guidance. I would like to express my appreciation for the sincere friendship and supportive advice from Loris, Arren, Jörn, and Nikhil. I like to think that my attitude has been shaped by their models. For the opportunity to learn and develop in the exciting environment of IIT and for the encouraging guidance, I am grateful to Prof. Caldwell. Genuine thanks also go to Prof. Medrano-Cerda, Wesley, Giacinto, Aaron, Andrea, and others who have endured many questions and whose participation has resulted in many engaging constructive discussions that have influenced this work. Practically, no achievement would have been possible without the interest and expert contributions of Marco, Paolo, and others who have con-

tributed to the development of our high-tech toys. Also, buying parts for these high-tech toys and traveling around to show them off has been possible thanks to the apparently infinite patience of Silvia, Valentina, Giulia and all the ADVR support team. I have been very fortunate to find authentic connections with colleagues, friends and fellow students Martijn, Sara, Veronica, Alperen, Cheng, Lorenzo, Matteo, Lucia, and many others with whom we shared the ups and downs of this intense journey. I am sincerly grateful for the friendship and the fun time shared at work with Jorge, Tommaso, Giovanni, Matteo, and Maria, who create the warm atmosphere in our group.

Thanks to my family for being my biggest inspiration and encouraging me to do my best. If in life I accomplish even a portion of what they have accomplished, I will consider it a great success.

A special final note is for Federica. Our feelings for one another make my life feel complete.

CONTENTS

1 Introduction

1.1 Motivation

Exoskeletons are wearable devices generally aimed at supporting physical tasks by generating appropriate forces on one or multiple human joints. Applications of exoskeletons cover a wide range of domains[1]. Medical exoskeletons may be used as part of clinical rehabilitation to help restore a motor function that was partially or entirely lost, or outside therapy to enable impaired people carry out activities of daily living. Lower-limb walking exoskeletons are perhaps the most prominent example [1, 2], associated to a growing number of commercially available devices. These include Lokomat[2], Ekso GT[3] and Indego[4]. With regards to able-bodied users, military research has produced a variety of devices aimed at reduc-

[1] A non-scientific but nonetheless helpful resource is the ExoskeletonReport.com catalog, which can be accessed at http://exoskeletonreport.com/product-category/exoskeleton-catalog/.

[2] https://www.hocoma.com/solutions/lokomat/

[3] http://eksobionics.com/eksohealth/products/

[4] http://www.indego.com/indego/en/Indego-Personal

ing effort and energy expenditure during demanding missions [3]. Also, the consumer market has most recently started to offer devices for use in sports practice. Examples are Ski-Mojo[5] and Againer[6], passive knee braces to assist skiing. Another recent trend, and focus of the present research work, is represented by applications in ergonomics for the workplace [4].

The development of exoskeletons poses significant technical challenges that are connected to the application. Compactness and low weight are a design goal common to most exoskeletons. Compactness promotes compatibility with human movements, daily-use equipment, and contributes to user acceptance. On the other hand, the extra mass added by a device is energetically expensive to accelerate, and it may additionally introduce undesirable dynamics and thus interaction forces, which may affect negatively the physical effectiveness as well as user acceptance. In contrast to stationary platforms used for clinical rehabilition, power autonomy is a goal for most mobile exoskeletons. Low energy consumption is therefore an important requirement to promote the success of a device in real environments. The aspects above are given primary importance in the work presented here.

There has been increasing interest in employing exoskeletons to reduce the physical loads on human workers carrying out demanding tasks. Manual material handling is a common demanding task in industrial scenarios (e.g. car and aerospace manufacturing, logistics, construction). This activity generates large compressive loads on the lumbar spine over $5000N$ and thus carries a high risk of physical injury [5]. In 2016, the Italian Workers' Compensation Authority (INAIL) reports[7] over 31000 new cases of

[5]http://www.skimojo.com/

[6]http://againer-ski.com/

[7]Data are taken from INAIL's open database, available at

absence from work due to musculoskeletal disorders (about 68% of the total cases of absence). A large part of these (42%) are associated to the spine, making it the area most subject to disorders. Among the causes, spine disorders are associated to longer absences compared to the overall average. Work-related injuries not only increase the costs sustained by companies, but most importantly have a severe impact on the workers quality of life. Safety and ergonomics guidelines for the workplace aim to reduce the workload on workers, often resulting in very strict limitations on the weights that can be handled depending on operating conditions such as frequency and posture [6, 7, 8]. These strict limitations give rise to opportunities for novel technical solutions, among which wearable exoskeletons have attracted great interest.

In early 2015 de Looze *et al* compiled a review on known exoskeletons for industry and their reported effect on the physical work load [4]. In association with different back-support exoskeletons, reduction in physical work load has been quite consistently documented. Passive devices have led to reductions in muscular activity ranging between 10% and 40%, mostly in simplified laboratory scenarios (e.g. in [9]). Also, reductions in lumbar compression forces up to around 25% have been estimated. These numbers establish convincing starting evidence of the potential effectiveness and encourage further development on back-support exoskeletons. In late 2017, at the time of writing the present manuscript, the review in [4] no longer provides a complete picture of the landscape of industrial exoskeletons. Over the last few years, a number of passive devices (the Laevo[8] and the BackX[9]) have established a position within the community

http://dati.inail.it/opendata/ (in Italian).

[8] `http://www.laevo.nl/`

[9] `http://www.suitx.com/backx`

as more and more possible applications are found and tested. However, their actual daily use in the field is not yet clearly demonstrated. On the other hand, new active exoskeletons have very recently made a strong appearance in the market (the Atoun Model A[10] and the Hyundai H-WEX[11]), as big companies have invested substantial resources in this sector. Due to their intrinsic versatility compared to passive systems, active exoskeletons hold the potential for even greater biomechanical benefits, although they are associated to significantly more complex designs. Their potential impact is still held back by substantial and open technological challenges. Additionally, standard validation methods are yet to be established within the community.

1.2 Objectives and approach

This thesis aims at addressing key challenges to advance the enabling technologies and ultimately foster the development of active exoskeletons, focusing on their practical use and translation into real-life scenarios. The research work is applied to an active back-support exoskeleton designed to assist repeated manual handling of heavy objects, but an attempt is made to generalize the findings to a broader range of applications. This exoskeleton aims at contributing with substantial forces on the torso so as to reduce the large compressive forces on the lumbar spine. The investigation focuses on some of the aspects that are considered particularly impactful and relevant to promote user acceptance of active exoskeletons, namely actuators and control strategies.

[10] http://atoun.co.jp/products/atoun-model-a

[11] https://www.hyundaipressoffice.co.uk/release/827/

Actuation

Actuators are the defining component of active exoskeletons. As greater forces and performance are required, they become increasingly heavy, compromising user comfort, and expensive, compromising market potential. Mechanical arrangements of motors and springs have the potential to improve on certain actuator features such as power or energy consumption. In this research work, a parallel arrangement is exploited to make more appropriate use of actuation resources than a comparable rigid actuator in generating the torque required for the task. This point is made by introducing a simplified model, based on which measures of dynamic performance are used to argue in favor of the parallel-elastic actuator.

Control strategy

Intuitive operation and smooth physical interaction are crucial to user acceptance of an active device, which places large importance on how its function is commanded and adjusted to generate meaningful assistance on its operator. Indeed this is also the key advantage of active exoskeletons, which may implement multiple strategies to target different tasks, as well as adapt them to different users and task conditions. This thesis explores the design of control strategies on a back-support exoskeleton aiming at seamless and intuitive operation. The proposed strategies rely on measurements of the user's posture as well as muscular activity.

1.3 Research context

The work presented here was carried out thanks to multiple larger projects. I was a member of the Marie Curie Initial Training Network (ITN) for Sustainable Manufacturing through Advanced Robotics Training Network in Europe (SMART-E). This consortium was supported by the European Commission under the FP7 program. Within this network, I belonged to the package on Safety and Human-Robot Interaction. The opportunities within this framework ranged from training on non-technical skills to expanding my network of connections at international events in the field. RoboMate, another EU-funded consortium active for the first two years of this three-year doctoral work, provided the context on industrial exoskeletons, on their most relevant technical challenges and on possible applications. Lastly, I have been involved in a newly-started three-year project funded by INAIL. This new enterprise sets out to further advance the development of exoskeletons for industrial applications, exploiting the strong and direct involvement of INAIL in measures for reducing workplace injuries.

1.4 Contributions

The first contribution of this doctoral thesis is an up-to-date overview of existing back-support exoskeletons with particular focus on the differences between passive and active devices. Following this overview, the overall concept of a prototype is illustrated. The core research contributions in the two areas of actuation and control strategy are described below. To complement the core contributions with evidence of the effectiveness of the prototype, validation methods and results are presented.

Actuation

- Development and description of a concept for a parallel-elastic actuator (PEA) to achieve the range of joint torques required by the target task.
- Description of a simplified actuator model and comparison of dynamic performance between the PEA and a rigid actuator.

Control strategy

- Development, implementation and testing of an indirect strategy based on user posture using information from the exoskeleton.
- Development, implementation and testing of a direct strategy based on unobtrusive electromyographic measurements.

1.5 Outline

Chapter 2 provides the necessary background to motivate and contextualize the technical challenges addressed in this thesis. It firstly introduces biomechanical models of the lumbar spine, used to describe compressive loads and the possible effect of exoskeletons on them. Secondly, it offers an up-to-date overview on existing back-support exoskeletons, including research prototypes and commercially available products, and with focus on the differences between passive and active devices.

Chapter 3 introduces a design rationale for choosing a parallel-elastic actuator (PEA) on the target back-support exoskeleton. A simplified model

and relative measures of dynamic performance are used to support the advantage of a PEA against a comparable rigid actuator.

Chapter 4 presents the implementation of different assistive strategies exploiting combinations of user posture and muscular activity to modulate the assistive forces generated by the exoskeleton. The discussion supports that the central advantage of active exoskeleton is the versatility to employ different strategies to target different tasks and conditions.

Chapter 5 complements the core contributions of this thesis by describing the methods for validation and some results of the experimental campaigns carried out on the prototype. The results in terms of reduced muscle activity are in line with the literature on comparable devices and provide encouraging evidence on the physical effectiveness.

Chapter 6 summarizes the findings of this thesis and discusses them with relevance to the technical challenges as well as their impact on future research and development of active exoskeletons.

2 Background

Summary This chapter provides the necessary background to motivate and contextualize the technical challenges addressed in this thesis. Biomechanical models of the lumbar spine are first introduced. They capture how large compression forces are generated as a result of external loads and the muscular activity that balances them. An extended model additionally represents the assistive action from a back-support exoskeleton and how it may reduce compressive loads on the lumbar spine. Secondly, an up-to-date overview of back-support exoskeletons is presented. The focus is on the advantages and drawbacks of passive and active devices. Finally, the prototype used in this research is described touching on its most salient features.

Parts of this chapter have been published as: **Toxiri, S.**, Ortiz, J., Masood, J., Fernández, J., Mateos, L. A., & Caldwell, D. G. (2015, December). A wearable device for reducing spinal loads during lifting tasks: Biomechanics and design concepts. In *Robotics and Biomimetics (ROBIO), 2015 IEEE International Conference on* (pp. 2295-2300). IEEE.

2.1 Biomechanics of lifting

This section addresses the biomechanical modeling of the lumbar spine in postures associated with lifting tasks. It aims at providing the necessary background on how a wearable assistive device may reduce spinal loads.

2.1.1 Prior work

The review article by Reeves *et al* [10] individuates some spine modeling categories. The so-called Link-Segment Models (LSMs) represent the human body as rigid links connected by ideal rotational joints, possibly featuring static and dynamic phenomena [11, 12]. While these models can lead to understanding of joint moments, they are not able to predict joint compressive reaction forces. Muscle Equivalent Models (MEMs) address this limitation by extending LSMs. They represent joint torques as generated by muscles along their anatomical line of action, assuming known lever arm about the corresponding joint. Muscles typically act with very short lever arms, which typically makes it necessary for them to develop very large forces to balance external loads. This is especially important in the lumbar spine, where the spinal muscles act only a few centimeters posterior to the vertebrae. As a consequence, a large part of the lumbar compression is generated by the spinal muscles themselves. In 1985, Chappin et al. [13] proposed a static biomechanical model of the lumbar spine. Their model accounts for gravity as well as for musculoskeletal forces can therefore be categorized as a static MEM. Similar biomechanical models have been employed to support the design of wearable assistive devices. For example, Naruse *et al* [14], adopted a static MEM to analytically show

that their prototype would reduce spinal loads. More recently, Luo *et al* [15] also formulated a similar problem to support the design of an assistive device. However, a central point in [10] is the importance of dynamics in estimating spinal loads, which may be increased by as much as three times. In the following, a dynamic MEM is employed to explore the effect of a back-support exoskeleton on reducing spinal loads.

2.1.2 Dynamic model

Fig. 2.1 illustrates the biomechanical model used in the present work. It is two-dimensional and features one main rigid body representing the human torso projected onto the sagittal plane, i.e. as seen from one side. The torso has mass W_T and is connected to ground via a rotational joint representing the lumbosacral joint. An additional mass W_L represents an external object held at the hands and is modeled as moving rigidly with the torso, at a constant distance d_L. While this weak assumption entirely neglects the movements of the arms, it fits the present objective of approximating the effect of a wearable device on the lumbar compression. The spinal muscles apply an additional force F_M to the torso, parallel to the torso and posterior to the rotational joint with a moment arm $d_M = 0.05m$ [10]. Therefore, they generate a torque opposite to gravity acting on the masses. The compression on the lumbar spine is represented by the component of the joint reaction force parallel to the torso, i.e. R_C.

The force generated by the spinal muscles and the lumbar compression can be calculated in this simple model by writing the dynamic equilibrium for the system above, as follows:

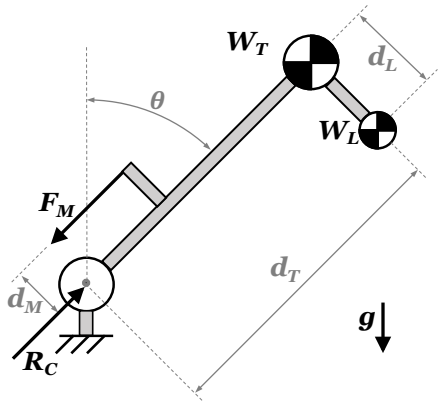

Figure 2.1: Two-dimensional biomechanical model of the lumbar spine on the sagittal plane. The rotational joint represents the lumbosacral junction. The torso and load have mass W_T and W_L. The angle θ represents the orientation of the torso with respect to the direction of gravity. The spinal muscles apply a force F_M on the torso at a distance d_M from the rotational joint. R_C represents the compression force on the lumbar spine.

$$\begin{aligned} F_M d_M = &+ gW_T d_T sin\theta \\ &+ gW_L\Big[d_T sin\theta + d_L sin(\theta + \tfrac{\pi}{2})\Big] \\ &- \big(J_T + J_L\big)\ddot{\theta} - d_L d_T \dot{\theta}^2 W_L \end{aligned} \tag{2.1}$$

$$R_C = F_M + g(W_T + W_L)cos\theta - d_T\dot{\theta}^2\big(W_T + W_L\big) \tag{2.2}$$

where θ is the orientation angle of the torso with respect to the direction of gravity, defined as zero corresponding to upright positions and positive for forward bending; F_M is the contraction force developed by the spinal muscles; R_C is the compression on the lumbar disc, represented by the joint reaction force along the spine; W_T and W_L are the masses of the

torso and the external load, respectively; d_M is the distance between the rotational joint and the line of action of the muscles; d_T is the distance of the center of mass of the torso from the rotational joint; d_L is the constant distance of the center of mass of the load from that of the torso.

Assistance: two possible configurations

As an extension of the model above, the idea of reducing the spinal loads by means of an assistive device is presented in the following. Two possible ways for delivering mechanical assistance are analytically compared. The two configurations are illustrated in Fig. 2.2.

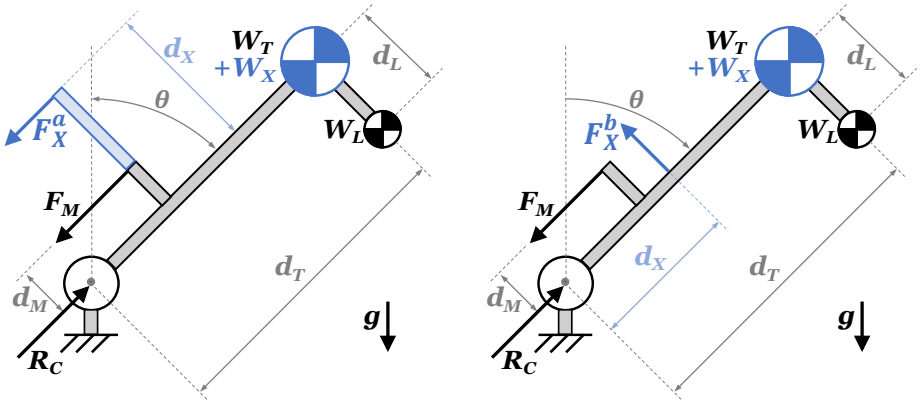

(a) Parallel (b) Perpendicular

Figure 2.2: Two possible configurations to provide mechanical assistance. On the left, the parallel configuration applies an assistive force along the line of action of the spinal muscles. The perpendicular configuration on the right applies the same force but oriented perpendicularly with respect to the spinal muscles.

In both cases, the device is modeled as an additional mass W_X that, for the sake of simplicity, is applied to the center of mass of the torso. Its assistive action is represented by a force F_X, the orientation of which is the key difference between the two configurations. Fig. 2.2(a) shows force F_X^a as acting through the lever arm of length d_X and in parallel with F_M. F_X^a is applied on an additional massless body, which is rigidly attached to the torso in this simplified model. The alternative option is depicted in Fig. 2.2(b), where F_M^b acts through a lever arm of equal length d_X but is perpendicular to the line of action of the spinal muscles.

$$\begin{aligned} F_M^a &= F_M - F_X^a \tfrac{d_X}{d_M} + gW_X d_T sin\theta \\ F_M^b &= F_M - F_X^b \tfrac{d_X}{d_M} + gW_X d_T sin\theta \end{aligned} \tag{2.3}$$

$$\begin{aligned} R_C^a = F_M^a + F_X^a \quad & +g(W_T + W_X + W_L)cos\theta + \\ & -d_T\dot{\theta}^2\big(W_T + W_X + W_L\big) \\ R_C^b = F_M^b + 0 \quad & +g(W_T + W_X + W_L)cos\theta + \\ & -d_T\dot{\theta}^2\big(W_T + W_X + W_L\big) \end{aligned} \tag{2.4}$$

Assuming $F_X^a = F_X^b$, Equation (2.3) suggests that the two options have the same effect of reducing the muscular force, resulting in $F_M^a = F_M^b$. However, the compression forces R_C^a and R_C^b in Equation (2.4) are not equal (see Fig. 2.3), due to the different orientations of F_X^a and F_X^b. The former, acting along the torso, contributes to compressing of the lumbar spine. The latter, while offering an equal assistive torque $F_X^b d_X = F_X^a d_X$, is directed perpendicular to the torso and thus does not contribute to compressing the lumbar spine[1]. This is illustrated in Fig. 2.3 showing the

[1]Rather, based on the model presented, the perpendicular configuration may increase

estimated compression force R_C, calculated based on Equation 2.4 in combination with motion data (as described in the next section) for the two configurations and different loads. This analysis suggests that the perpendicular configuration in Fig. 2.2(b) is preferable to the parallel configuration in Fig. 2.2(a). The former is therefore adopted in the following part of this work, which therefore considers $F_X = F_X^b$.

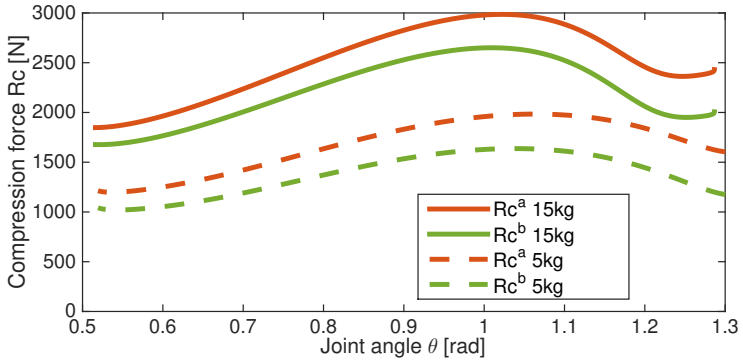

Figure 2.3: Estimated lumbar compression force R_C (Equation 2.4 in combination with motion data, as described in the next section) against torso orientation, calculated with real motion data for the two different configurations. The green and orange lines refer to the perpendicular and parallel configurations, respectively. The mass of the load being moved is $5kg$ or $15kg$ (see legend). Greater compression forces can be observed in associated to the parallel configuration.

shear (as opposed to compressive) loads on the lumbar vertebrae, but the effect of these is not covered in this work.

Comparative analysis of spinal loads

The models above are employed to compare the estimated spinal loads in two scenarios: unassisted, i.e. with no exoskeletons, and assisted via the perpendicular configuration in Fig. 2.2(b).

The mass of the device is conservatively assumed to be $15kg$. For the sake of this analysis, the assistive force is implemented as proportional to the orientation angle of the torso to represent the implementation of an ideal rotational spring, as in Equation (2.5). The model parameters are summarized in Table 2.1.

$$F_X = G_X \cdot \theta \tag{2.5}$$

The comparison is carried out between the unassisted model in Fig. 2.1 and the assisted one in Fig. 2.2(b). The output variable of interest is the estimated lumbar compression forces R_C and R_C^b, calculated using Equations 2.2 and 2.4, respectively. This quantity is estimated using load mass (W_L) and motion (θ, $\dot{\theta}$ and $\ddot{\theta}$) extracted from experimental data provided by our project partner TNO[2]. During these experiments, subjects were asked to start at an upright posture, bend forward to grab an object from the ground, move the object onto a table, and the same in the opposite order. Objects of mass 0, 5, 10 or $15kg$ were used. The motion data for distinct task executions are illustrated in Fig. 2.4.

Fig. 2.5 shows the estimates of the spinal compression, computed based on the equations introduced previously. The assistance uniformly reduces the compression forces on the spine. Particularly large reduction is observed corresponding to greater orientation angles of the torso. This ana-

[2]Nederlandse Organisatie voor Toegepast Natuurwetenschappelijk Onderzoek, https://www.tno.nl/en/

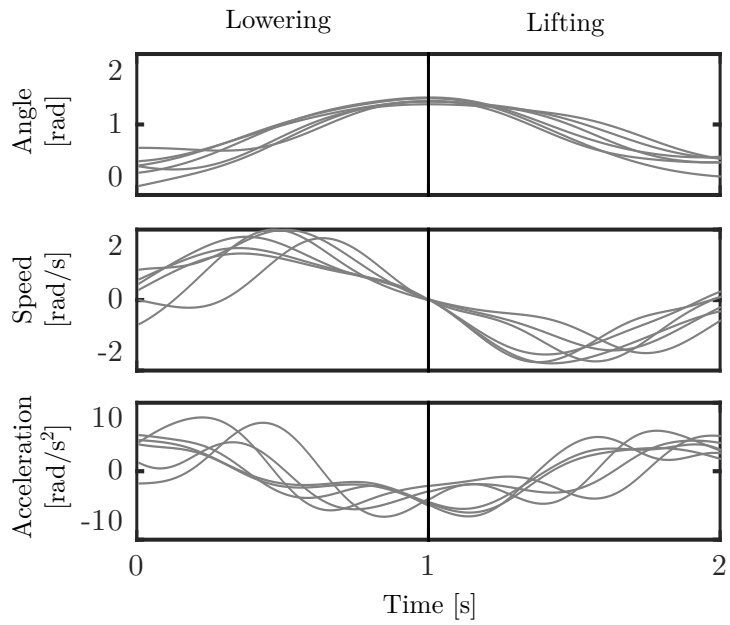

Figure 2.4: Motion data for distinct executions of lifting and lowering movements. The angle represents the orientation of the torso with respect to the direction of gravity.

Symbol	**Description**	**Value**	**Unit**
g	Gravity	9.81	$[m/s^2]$
W_T	Torso mass	50	[kg]
W_X	Device mass	15	[kg]
d_M	Spinal muscle lever arm	0.05	[m]
d_T	Distance torso CoM - joint	0.313	[m]
d_L	Distance load - torso CoM	0.25	[m]
d_X	Distance spine - F_X	0.3	[m]
G_X	Proportional gain	330	$[Nm/rad]$

Table 2.1: Model parameters.

lysis also supports that as the external load increases, larger lumbar compression forces are generated.

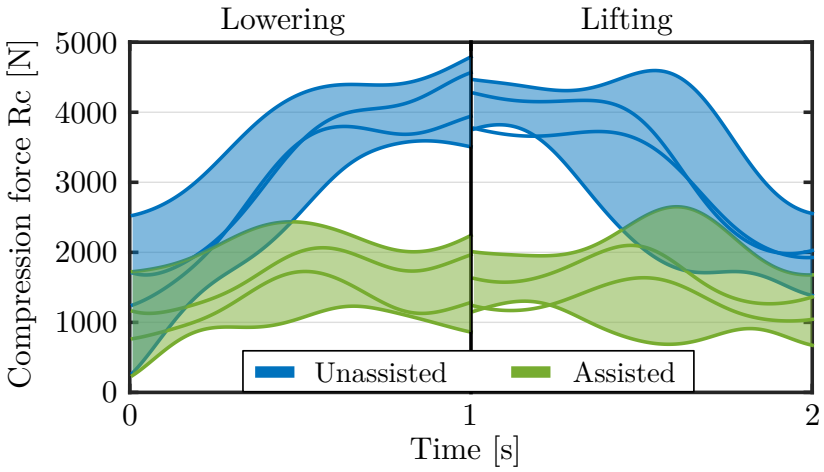

Figure 2.5: Estimated lumbar compression force R_C (Equations 2.2 and 2.4), calculated with real motion data corresponding to lowering and lifting loads. The blue area and lines refer to the unassisted scenario, while the green shows the reduction in the compression when assistance is provided. The mass of the load being moved varies between 0 and $15kg$, corresponding to generally higher compression forces.

Considerations

The scope and some limitations of the model presented above are important to consider at this point. First of all, it is outside the scope of the analysis above to achieve accurate estimates of the lumbar compression. Rather, the aim is to qualitatively observe the potential effect of a proposed wearable assistive device. A big assumption associated to the modelling approach is to consider the pelvis as mechanically grounded and the up-

per body as rotating relative to the pelvis. Despite this simplification, the spinal muscles are appropriately represented as acting in parallel to the spine. Additionally, [10] warns about the sensitivity to variability in muscle lever arm. This is a concern in absolute terms but should not affect the relative estimate between the unassisted and assisted scenarios in Fig. 2.5.

2.2 Back-support exoskeletons: state of the art

The landscape of exoskeletons for industrial applications has expanded substantially in recent years. Back-support devices for manual handling tasks have attracted particular attention. Most back-support exoskeletons are built around the same concept: forces are generated between the user's torso and thighs to assist the extension of the back and hip joints. As a result, the muscular activity at the lower back is expected to be reduced. Concurrently, the compressive loads should decrease and thereby the associated risk of injury. In 2015, de Looze *et al* compiled a comprehensive review on scientific studies reporting the biomechanical effects of existing exoskeletons for industry [4]. In late 2017, at the time of writing the present manuscript, their review no longer provides a complete picture on the landscape of industrial back-support exoskeletons. It is thus helpful to contextualize the present doctoral research work by offering an updated overview on the most relevant examples of back-support exoskeletons, including research prototypes and commercial products. The first necessary distinction is between passive and active devices. Passive exoskeletons generate assistance by using mechanical springs, while active ones employ actuators (in most cases, these are electromagnetic gear motors).

2.2.1 Passive exoskeletons

Passive devices generate assistive forces by means of elastic elements only. In general, the elastic elements accumulate energy as the person moves from an upright position towards and bent posture. A number of prototypes and products have been proposed over the last years. Two types

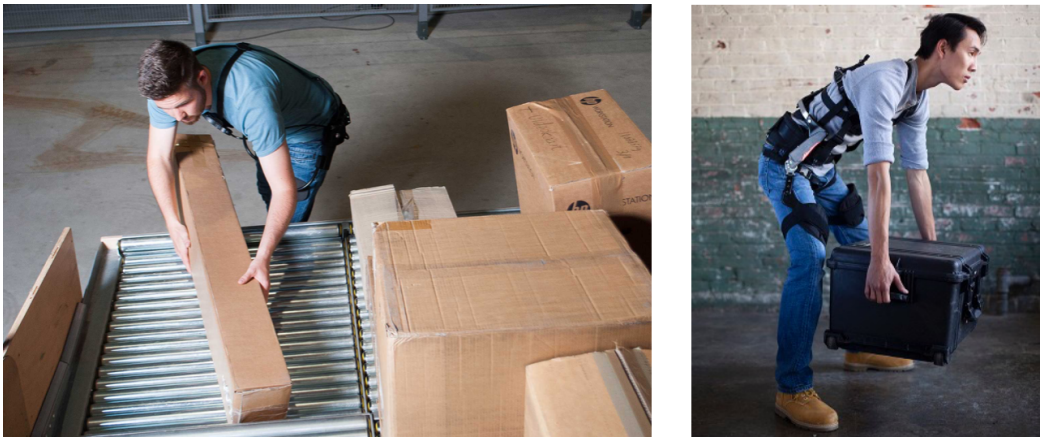

Figure 2.6: Left: Laevo (Image downloaded from: http://en.laevo.nl/); right: BackX (Image downloaded from: http://www.suitx.com/backx). Both are commercial, lightweight passive exoskeletons designed to support the lower back in unergonomic postures and during manual handling.

can be distinguished, depending on whether the assistive forces are transmitted to the user via a parallel rigid structure or directly to the body segments. The latter type can be considered soft and includes the PLAD (Personal Lift Assistive Device) and the SSL (Smart Suit Lite). The PLAD consists of elastic strings that run parallel to the human spine and thighs and, between the two, routed via pulleys [16]. The SSL, on the other hand, is implemented with wide elastic bands [17]. Perhaps the first passive exoskeleton using a rigid structure was the WMRD (Wearable Moment Restoring Device) from UC Berkeley [18]. It generates forces via a coil spring and transmitted them via strings as moments approximately about the hip joint. As the device connects to the ground via dedicated structures, its weight does not generate unwanted pressure on its wearer. The

BNDR (Bending Non-Demand Return) uses rotational springs mounted directly at the joint, it is secured to the user via a waist belt and transmits forces via padded rigid structures on the chest and thighs [19]. A similar implementation can be found on a recent commercial product, Laevo[3], which entered the market in 2015. Following a similar concept, BackX[4] was announced in 2016 as one module of an exoskeleton assisting the knee and shoulders as well. Most recently, the SPEXOR European research consortium set out to design a novel passive spinal exoskeleton with particular attention to allowing unrestricted movements and minimizing the unwanted effects of joints misalignment [20, 21, 22].

The elastic forces in passive devices are designed such that the weight of the user's torso is partially compensated during the forward bending motions in lifting tasks. As they are generated by passive elements only, these forces cannot be modulated during operation, which may limit the versatility of this class of exoskeletons. Additionally, their strength must be limited by design so as not overcompensate the user's own weight and excessively hinder movements.

2.2.2 Active exoskeletons

Active back-support exoskeletons appear to have developed in Asia more than elsewhere. Two currently commercial models started as research prototypes. Muscle Suit, by the Japanese Innophys CO, LTD[5] [23], uses pneumatic actuation and includes a small tank to store compressed air. The user can trigger its operation by either blowing into a dedicated mouthpiece or

[3] http://en.laevo.nl/

[4] http://www.suitx.com/backx

[5] https://innophys.jp/

Name		Technology	Structure	Parts of body
PLAD [16]	Research	Elastic strings, pulleys	Soft	Torso, calves
SSL [17]	Research	Wide elastic bands	Soft	Torso, thighs
WMRD [18]	Research	Coil spring, strings	Rigid	Torso, thighs, feet
BNDR [19]	Research	Leaf springs	Rigid	Chest, waist, thighs
Laevo	Product	Gas springs	Rigid	Chest, waist, thighs
BackX	Product	N.A.	Rigid	Torso, waist, thighs
SPEXOR [22]	Research	N.A.	Articulated	N.A.

Table 2.2: Summary of passive exoskeletons and their main features.

Figure 2.7: Left: Muscle Suit (Image downloaded from: `https://innophys.jp/about/`); right: HAL Lumbar Support (Image downloaded from: `http://exoskeletonreport.com/product/hal-for-lumbar-support/`). They are active exoskeletons, now commercial products resulting from years of scientific research at Japanese universities.

by pressing on a pad located between chin and chest. HAL (Hybrid As-

sistive Limb) Lumbar Support is a product of Cyberdyne[6], the Japanese company that also designs HAL as a full body exoskeleton. It is a compact device resting on the waist and actuated by electromagnetic motors. Electromyography on the spinal muscles is acquired to modulate the assistance provided [24]. Two more devices have recently made the market

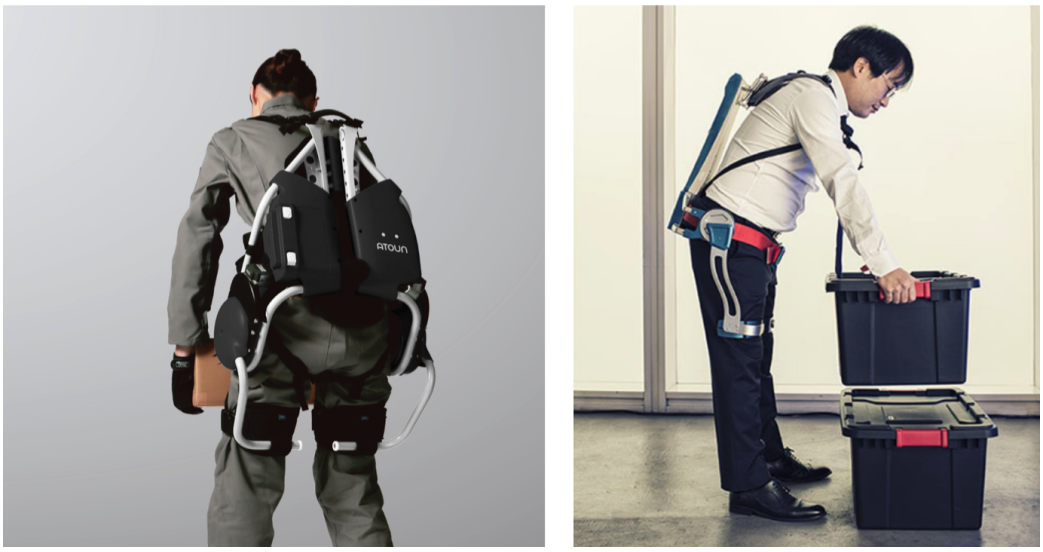

Figure 2.8: Left: Atoun Model A (Image downloaded from: `http://atoun.co.jp/products/atoun-model-a`); right: Hyundai H-WEX (Image downloaded from: `https://www.hyundaipressoffice.co.uk/release/827/`). They appeared in the market more recently than others.

in Asia. The first one, Atoun Model A[7], is backed by the Japanese Panasonic, which has been working on exoskeletons for some time. The device is actuated by two motors and battery powered. On the Korean Hyundai

[6] `https://www.cyberdyne.jp/english/`
[7] `http://atoun.co.jp/products/atoun-model-a`

H-WEX[8] (Hyundai Waist EXoskeleton), on the other hand, only one motor provides power to assist the back. Unfortunately, very little technical information is publicly available. Also, due to their very recent appearance, no results of rigorous of testing campaigns is available. A recent development on the European side is German Bionic[9], a young company that aims to exploit part of the results from the Robo-Mate EU research consortium[10] (further discussed in the Section 2.3). The HuMan[11] European consortium also has been addressing the development of exoskeletons for the support of industrial lifting, although no detail was found at the time of writing.

In contrast with the predetermined action of a passive exoskeleton, the forces exerted by active devices are commanded according to appropriate assistive strategies and can thus be modulated during operation and adjusted to different tasks and users. This represents the central advantage of active exoskeletons, which are believed to potentially bring greater reductions in joint loadings than passive devices. Different user interfaces have been proposed, ranging from EMG to the more unusual mouthpiece. At this stage it is unclear whether one is better than the others or which is more suited to the different possible target tasks.

[8] `https://www.hyundaipressoffice.co.uk/release/827/`
[9] `https://www.germanbionic.com/`
[10] `http://www.robo-mate.eu`
[11] `http://www.humanmanufacturing.eu`

Name		Technology	Command
Muscle Suit [23]	Res./Prod.	Pneumatic	Mouthpiece, chin pad
HAL Lumbar Support [24]	Res./Prod.	EM motors	EMG at lower-back
Atoun Model A	Product	EM motors	N.A.
Hyundai H-WEX	Product	N.A.	N.A.
GermanBionic CRAY	Product	EM motors	Inclination
HuMan EU project	Research	N.A.	N.A.

Table 2.3: Summary of active exoskeletons and their main features.

2.3 The *Robo-Mate* Mk2 prototype

The device used in this work is an active back-support exoskeleton. Its development was supported by the EU-funded FP7 project Robo-Mate[12] [25] and has later continued via national funding by INAIL (the Italian Workers' Compensation Authority). This section describes the details of its second version, named Mk2. A more recent, slightly refined version (Mk2b) is available at the time of writing, but for the sake of consistency across chapters a description of Mk2 is preferred. With reference to the overview in the previous section, some central overall objectives and respective design choices are summarized as follows.

- It should produce forces that substantially contribute to back and hip extension. A rigid structural frame complemented with padded straps from a commercial backpack were chosen to withstand large forces safely and transfer them comfortably to the body segments of interest (Section 2.3.1).

- It should be lightweight, portable, and have low footprint. Electro-

[12] http://www.robo-mate.eu

magnetic motors were chosen as a good compromise between compactness, portability and weight (Section 2.3.2).

- It should allow unhindered movements. A joint torque sensor was embedded in each actuation unit to ensure appropriate control accuracy and precision at low torques (Chapter 3). Additionally, a number of passive degrees of freedom were included as part of the connecting links to allow unrestricted movements outside the actuated joints (Section 2.3.1).

- It should result in seamless assistive action. Different strategies were explored aiming at minimal obtrusiveness and intuitiveness for the user (Chapter 4).

2.3.1 Structures

The prototype, represented in Fig. 2.3, spans the torso and upper legs similarly to most of the devices described in Section 2.2. On the torso, it is attached via parts of a commercial backpack, including shoulder straps with front clip, a wide waist band, and a padded rigid plate at the lower back. Custom Velcro-bands to fix the leg links to the thighs were sewn in-house. Attached on the rigid back plate is a custom-designed rigid frame that holds the two actuators in place, one on each side lateral to the hip joint and approximately aligned with its axis of flexion-extension. During the donning procedure an assistant attempts to align the actuator at the hip, and subsequently the multiple adjustment straps are used to distribute weight and pressure to the user's preference. Each actuator generates torque between the rigid frame and the corresponding thigh link. The

Figure 2.9: Side view of the *Mk2* prototype.

torque is approximately limited to the sagittal plane. The leg links connecting each actuator to the corresponding thigh band are endowed with a set of five passive degrees of freedom [26]. Additionally, the shoulder

straps are connected to the rigid frame via a spherical joint providing three additional passive degrees of freedom. These ensure that user movements are unhindered (e.g. twisting the torso; hip abduction and adduction; hip internal and external rotation) and as a result promote comfort.

2.3.2 Actuators and electronics

Each actuation unit includes a brushless DC motor coupled to a compact reduction gear. In parallel with the gear is a custom rotational spring, based to the concept of parallel-elastic actuation (PEA). The implementation of the parallel spring is described in Chapter 3. The total joint torque produced by the two elements is measured via a commercial, strain gauge-based joint torque sensor. Table 2.4 provides details on the components of the actuator.

Motor	-	Maxon EC60 flat 24V
Motor driver	-	Maxon ESCON 50/5 Module
Nominal power	W	100
Nominal torque	mNm	289
HarmonicDrive gear	-	SHD-20-100-2SH
Reduction ratio	-	100
Torque sensor	-	ME-Systeme TS110a

Table 2.4: Table summarizing the actuator components and specifications.

All the electronics and computers are located in a custom plastic box, fit on the custom rigid frame near the back plate. The cables connecting the electronics to the motors and torque sensor are routed through the hollow profiles constituting the rigid frame. Commercial components in-

clude: the driver for the brushless motor (Maxon ESCON 50/5 Module); the main computer in charge of the custom control software and communications (Intel NUC); inertial measurement unit (IMU), mounted on the rigid frame (xSens MTi-30 AHRS). Custom electronics include: the amplification and digitalization of the signal acquired via the torque sensor; various breakout and connection boards. At the present stage the exoskeleton still relies on external power supply, although future plans to include a battery have been made.

2.3.3 Controls

The control scheme is structured on two levels, as depicted in Figure 2.10. The general goal of this scheme is that the user is free to move as intended and additionally experiences substantial assistive forces with appropriate timing and extent. This concept has been referred to as *following user intention*. On the low level, a closed-loop torque controller is in charge of tracking the reference torque signal at each actuator. A description of the closed-loop controller regulating the torque at the corresponding actuator is provided in Chapter 3 and therefore omitted in this section. A high level strategy establishes the necessary amount of assistive torque and generates a reference signal accordingly, based on bioelectrical and biomechanical measurements. No further details are presented in this section, as this aspect is expanded in Chapter 4. This control scheme is implemented in C++ and is executed at $1kHz$ by the main on-board computer.

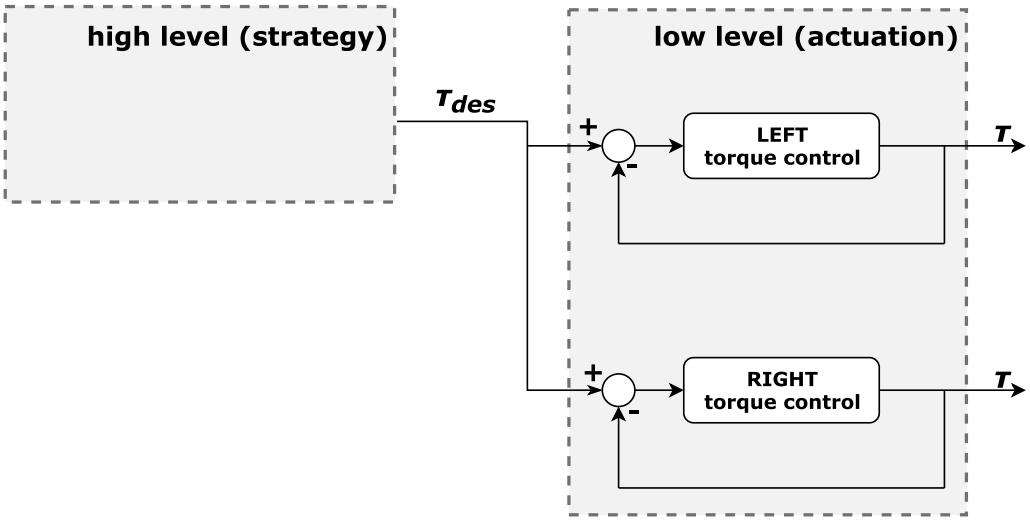

Figure 2.10: The implemented control scheme, articulated in two levels. The low level regulates the torque output at the actuators. The high level corresponds to the assistive strategy and is responsible for the extent and timing of the generated assistance.

3 PARALLEL-ELASTIC ACTUATION

Summary Actuators are the defining component of active exoskeletons. As greater forces and performance are required, they become increasingly heavy and expensive. The design rationale for a parallel-elastic actuator (PEA) is proposed to match the asymmetrical torque requirements associated to the target task. In this case, a PEA makes better use of the motor operating range. A simplified actuator model and relative performance measures are presented to suggest that, thanks to the parallel spring, a more convenient choice for the motor can be made. This leads to improved dynamic performance as captured by the proposed measures, which are associated to user comfort and are thus considered to promote user acceptance in the workplace.

Parts of this chapter have been published as: **Toxiri, S.**, Calanca, A., Ortiz, J., Fiorini, P., & Caldwell, D. G. (2017). A parallel-elastic actuator for a torque-controlled back-support exoskeleton. *IEEE Robotics and Automation Letters*, 3(1), 492-499.

3.1 Introduction

When designing an exoskeleton, it is important to keep its weight as low as possible to promote comfort during use. By contrast, generating large assistive forces tends to require heavy components. As a result, the design trade-off between weight and forces is of special importance. Furthermore, the actuators typically make up a significant portion of an exoskeleton's weight, which makes their design of particular interest.

Electromagnetic motors are the most common type of actuators on exoskeletons, but high-reduction gears are typically required to achieve large joint torques. As a result, the torque-to-weight ratio and the achievable torque-control performance are often compromised. It is therefore important to consider the task dynamics when defining the actuation requirements to avoid overdimensioning the motor and gearbox. Instead of using motors, it is also possible to generate assistive forces employing only passive elements such as mechanical springs. Exoskeletons of this type (known as passive) are typically simpler in their design, more lightweight and do not require electrical power, but their versatility and functionalities are limited compared to those with actuators. Parallel mechanical arrangements of motors and springs have been proposed to combine the benefits of the two solutions [27, 28, 29, 30].

As introduced in Section 2.3, an asymmetrical torque range is associated to the requirements for the target back-support exoskeleton. With reference to the mechanical spring-motor arrangements mentioned above, this chapter illustrates the rationale for choosing a parallel-elastic actuator (PEA) to generate the necessary torques. The design of the PEA is elaborated based on the task requirements, allowing the convenient choice of a

lower-inertia motor-gear, which is associated to improved torque-control performance. This improvement is formally analyzed and experimentally validated.

3.1.1 Prior work

To combine the versatility of motors with the energetic convenience of springs as torque source on robotic devices, different mechanical arrangements have been proposed in the literature. Among the key drivers, reducing energy consumption and maximum motor power and torque requirements have played an important role.

A study on elastic actuators for lower-limb exoskeletons found the parallel configuration to be beneficial for the hip and ankle joints during walking [27]. An asymmetric two-branch actuator designed for energy efficient robotic joints was presented in [28, 31]. This concept can be seen as a parallel-elastic actuator, where the parallel elastic branch contributes to joint power by storing significant amounts of energy. The energy efficiency associated to parallel elastic branches was also studied with specific application in walking with ankle prostheses [29]. Additional insights into the dynamics and energetics of elastic actuators were recently given in [32]. The energy-saving property of parallel elasticity emerged in an experimental study with the HAL Lumbar Support [33]. In [30], the parallel-elastic branch was explicitly used to reduce the motor torque requirements in an actuated ankle prosthesis. Indeed, the parallel configuration makes better use of the motor operating range in the case of asymmetric torque requirements [34].

Considering the application field of exoskeletons, this approach is focused on torque-control performance as opposed to energy efficiency. The

former is strongly associated to user experience and comfort. To this aim, Series-Elastic Actuators (SEAs) have been proposed to improve torque control by reducing output stiffness [35]. PEAs, on the other hand, enable designs with lower reflected inertia, which is the focus of this chapter. The presented analysis uses simplified models to capture the effects on torque dynamics associated to different inertias.

3.2 Design concept

The physical task targeted by our exoskeleton is the repeated manual handling of objects up to $15kg$ in industrial scenarios. As described in [26], based on a biomechanical model and human motion data, it is estimated using inverse dynamics that the human body generates over $200Nm$ to extend lower back and hips, at joints speeds reaching $2rad/s$. Unsurprisingly, mostly torques against gravity are required to accomplish the tasks. Considering the goal of reducing the spinal loads and thus reducing the risk of injury, the exoskeleton was designed aiming to provide about half of the necessary joint torque ($100Nm$), leaving the rest to its user. Aiming to generate only a portion of the total torque[1] was a design decision meant to make the device safe to interact and never strong enough to physically overcome its user. It follows that the target for each of the two actuators is to accurately generate from very low torques up to about $50Nm$, depending on the situation and based on an appropriate assistive strategy.

As anticipated, the required torques are in nearly all cases positive, i.e. against gravity. Any traditional actuator would thus be overdimensioned, as its negative torques are not required to accomplish the physical task.

[1] The torque necessary to accomplish the task

Loosely speaking, a parallel spring helps by producing a portion of the torque at the joint, thereby offsetting the working space of the motor-gear to more closely match the asymmetrical range of required torques. It follows that the torque requirement for the motor-gear pair can be relaxed substantially, which given a similar power demand is expected to benefit in terms of maximum speed and dynamic performance. This aspect is expanded in the next sections.

In a previous iteration (from here on, Mk1), the actuators had been designed to achieve over $50Nm$ but with proved too slow for the target task. Motivated by this realization, the parallel spring was introduced as part of the following design (Mk2), which achieves significantly faster dynamics although with slightly sacrificed torque capabilities (under $50Nm$). However, the reduced torque range is due the specific parallel spring available when Mk2 was designed (more details later in this chapter), and may easily be increased with a stiffer physical spring.

The total torque capability of the PEA may be described qualitatively as depending on the spring deflection angle, i.e. the spring torque-deflection profile. At any given deflection, the range of possible output torques can be visualised as the motor-gear capabilities displaced by the spring profile. Fig. 3.1 conceptually illustrates the motor-gear working areas corresponding to two key configurations. In (a) the spring is in its resting position and thus produces no torque. The resulting actuator working area, described by the nominal torque and speed, is symmetrical and covers positive and negative torques in equal magnitude. The spring is designed such that its resting position corresponds to full extension of the user's torso and leg, which corresponds to where lowest torques from the exoskeletons are required. In (b) the spring is loaded such that its torque is about as large as

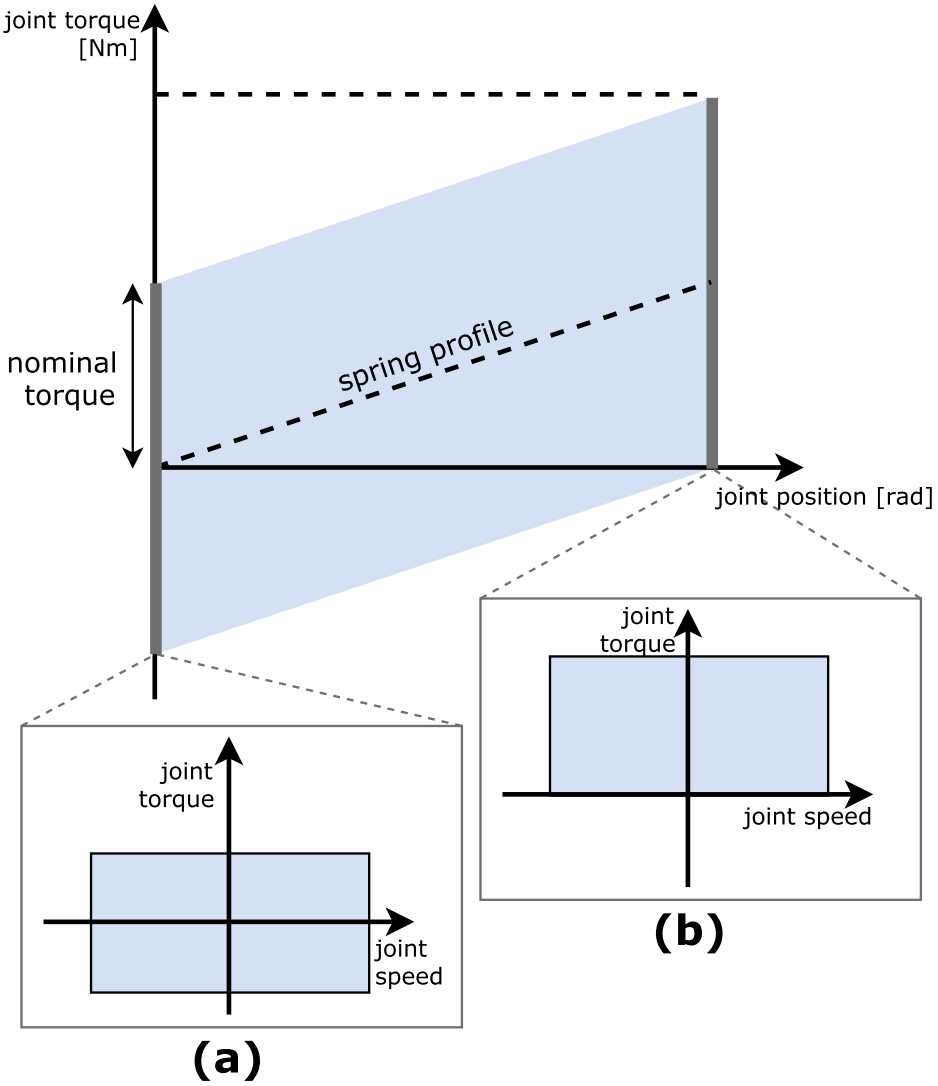

Figure 3.1: Illustration of the actuator working areas at two different spring deflection states. In (a) the spring is in its resting state, therefore the available torque range is symmetrical. In (b) the spring generates a torque about as large as the motor-gear nominal torque. The available torque range is therefore shifted to positive values only.

the motor-gear nominal torque. As a result, the range of possible torque outputs spans from around zero to twice the nominal torque. The spring is designed such that this configuration corresponds to the maximum joint angle between torso and leg, at which the torques required from the exoskeleton are largest. In other words, the parallel spring approximately doubles the maximum torque capabilities of the motor-gear pair in (b), where the requirements are most demanding. As a possible alternative to the parallel spring, choosing a gear with double the reduction ratio would also achieve double the maximum torque capabilities. However, this would additionally reduce the achievable joint speeds and negatively impact the torque-control performance due to much larger reflected inertias. Additionally, it would cover the negative torque range, which is largely unnecessary for the target task. It is also important to note that the spring is designed such that it is never stronger than the motor-gear pair. Its elastic torque can thus be compensated in any situation making it transparent to the user.

3.2.1 Physical implementation

The spring is implemented as an arrangement of an elastic cord routed in between poles, as illustrated in Fig. 3.2. Its design is outside the scope of this thesis and was introduced in [36]. This mechanism allows to achieve different joint stiffness values by selecting cords of different cross section. The result is a compact actuation unit that includes the motor, the reduction gear, the spring with associated mechanisms, and the joint torque sensor.

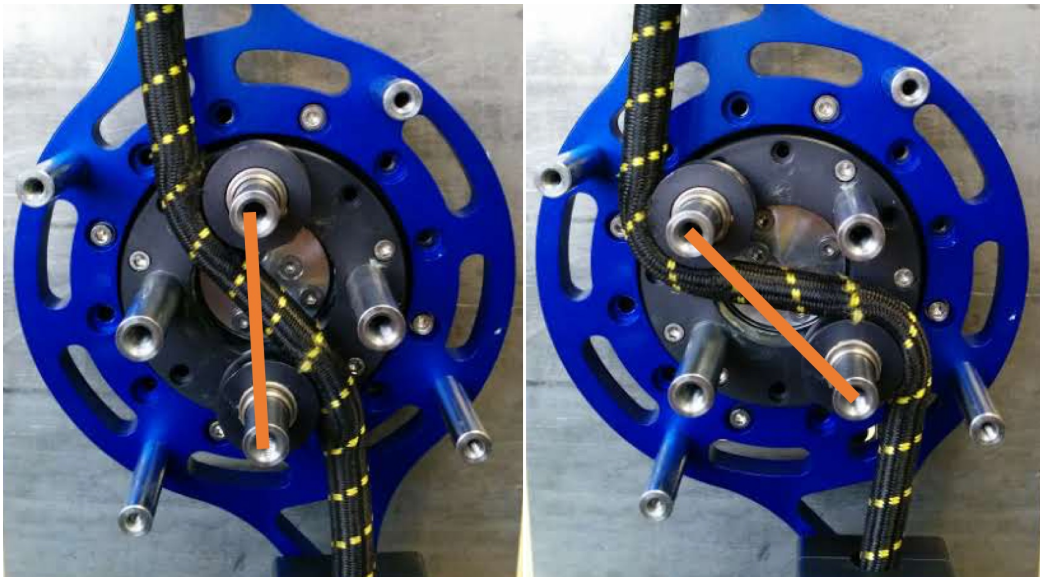

Figure 3.2: The implementation of the mechanical spring, in two configurations. On the left, the bungee is unloaded and it produces no torque on the joint. On the right, the joint is displaced by about 45 degrees and the bungee cord therefore produces a torque on the joint.

3.3 Actuator dynamics and control

3.3.1 Simplified dynamic model

Here a dynamic model of the actuator is presented. Under a number of simplifying assumptions, the model attempts to capture the dominant phenomena that determine torque dynamics. The simplifications at this stage include: (a) neglecting the dynamics of the low-level controller for the motor current; (b) considering the gearbox as infinitely stiff and therefore considering it as a rigid transmission. While this reduces the general

validity of the model, the focus is on a simplified analysis allowing more immediate interpretation.

Based on the above assumptions, the following model for a PEA-driven exoskeleton joint is considered:

$$(J_{mg}r^2 + J_l)\ddot{\theta} + d_v\dot{\theta} + d_c\text{sign}\dot{\theta} + k_p\theta = \tau_m - \tau_h \tag{3.1}$$

where θ is the angular position of the joint, J_{mg} is the sum of motor and gearbox inertias, r is the gear ratio, J_l is the inertia of the exoskeleton link between the actuator and the attachment to the user's thigh, k_p represents the stiffness of the parallel spring, while d_v and d_c represent the overall viscous and Coulomb friction parameters, respectively. The motor is controlled in current mode and τ_m is the motor input torque (proportional to the current) whereas τ_h is the interaction torque with the environment, measured using a torque sensor located at the output, such that it measures the sum of elastic and actuator torque.

3.3.2 Closed-loop torque controller

A control law is implemented including a proportional-derivative torque feedback supplemented by a feed-forward action, meant to reduce steady-state error. The term u attempts to compensate the large Coulomb and viscous friction typically introduced by the gear, in order to mask it from the user and thus promote comfort. The parallel spring is also masked from the user by the term u as follows.

$$\tau_m = u - P(\tau_h - \tau_{ref}) - D\dot{\tau}_h + \tau_{ref} \tag{3.2}$$

$$u = \hat{d}_v\dot{\theta} + \hat{d}_c\text{sign}\dot{\theta} + \hat{k}_p\theta \tag{3.3}$$

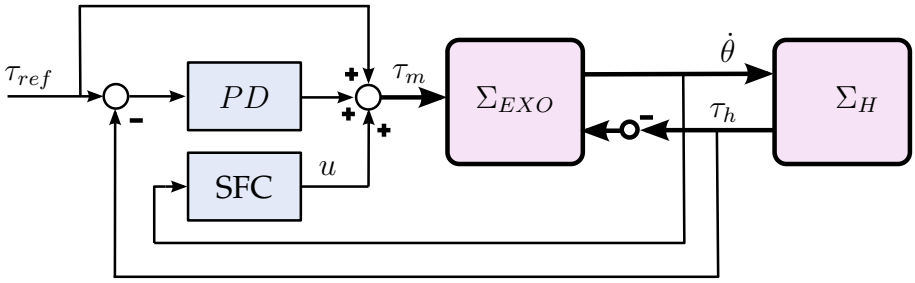

Figure 3.3: Block diagram representation of the controlled actuator. One can see the feedback interconnection of the control, the exoskeleton Σ_{EXO} and the human Σ_H.

where P and D are positive proportional and derivative gains, $\hat{d}_v$, $\hat{d}_c$ and $\hat{k}_p$ represent (under-) estimation of the parameters d_v, d_c and k_p, such that $\tilde{d}_v = d_v - \hat{d}_v > 0$, $\tilde{d}_c = d_c - \hat{d}_c > 0$ and $\tilde{k}_p = k_p - \hat{k}_p > 0$ to avoid over-compensating friction and spring stiffness. A graphical representation of the control scheme is proposed in Fig. 3.3 where the block SFC represents the stiffness and friction compensator given by u in Equation (3.3). The blocks Σ_{EXO} and Σ_H represents the exoskeleton (as an admittance) and the human (as an impedance) which are mechanically interconnected.

Considering the control law in Equations (3.2)-(3.3) applied to the system in Equation (3.1), the closed-loop dynamics become:

$$\frac{J_r}{P+1}\ddot{\theta} + \frac{\tilde{d}_v}{P+1}\dot{\theta} + \frac{\tilde{d}_c}{P+1}\text{sign}\dot{\theta} + \frac{\tilde{k}_p}{P+1}\theta + \frac{D}{P+1}\dot{\tau}_h = \tau_{ref} - \tau_h \tag{3.4}$$

where

$$J_r = J_{mg}r^2 + J_l \tag{3.5}$$

is the overall reflected inertia and parameters $\tilde{d}_v$, $\tilde{d}_c$ and $\tilde{k}_p$ are positive and reasonably small. The reader can notice that the parallel elasticity is not only compensated using the term $\hat{k}_p\theta$ (leading to the residual stiffness $\tilde{k}_p$)

but also masked using torque feedback which further reduces the residual stiffness by a factor of $P+1$. We highlight that this achievement is allowed by the specific torque sensor arrangement (in series with the parallel of spring and gearbox) which allows to not only mask the motor but also the spring dynamics by means of torque feedback. Thus, neglecting the less significant terms, the dynamics in Equation (3.4) becomes:

$$\frac{J_r}{P+1}\ddot{\theta} + \frac{D}{P+1}\dot{\tau}_h \simeq \tau_{ref} - \tau_h \tag{3.6}$$

Stability It is important at this point to consider that the discrete-time implementation of the controller in Equation (3.2) has an upper limit on the proportional gain. The upper limit is associated to the stability of a proportional force controller and is known from Whitney [37]. The limit value is determined by a combination of environment stiffness and sampling time:

$$P < \frac{1}{k_e \cdot T} \tag{3.7}$$

where T is sampling time and k_e represents the environment stiffness, at the output of the actuator. The value of k_e captures the stiffness of the deformable human tissues on the limb onto which the assistive force is applied (e.g. the user's thighs as shown in Fig. 2.3), as well as the stiffness of the link that connects it to the actuator. In general, the environment stiffness k_e may vary substantially during use, for example due to muscle contraction. While an accurate estimate of the limit value is outside the scope of the present study, it must be noted here that the value is independent of the actuator's dynamical properties. Therefore, in the remaining part it is assumed that the same limit applies to different actuators and thus use the same control gain on two different setups, which act on the same environment and are controlled at the same frequency (i.e. $1kHz$).

3.4 Comparative evaluation

In this section a comparison between the latest actuator in our prototype (Mk2, based on the PEA concept described above) and the actuator in the previous prototype (Mk1, based on a traditional design with no parallel elasticity and employing motor and gearbox only) is presented. The physical parameters of the two actuators are summarized in Table 3.1. As described in Section 3.2, the parallel elasticity in Mk2 allows the choice of a lower-torque motor and lower-reduction gearbox compared to Mk1, which results in lower reflected inertia J_r. Due to the same differences, Mk2 is also capable of working at greater joint velocities, while it should be noted that both Mk1 and Mk2 are capable of covering the asymmetrical range of torques required for the exoskeleton (specifically, Mk1 covers a wider, symmetrical range).

Torque performance are evaluated in relative terms in order to highlight the improvement associated to the implementation with parallel elasticity. A description of the experimental setups is provided first, followed by the introduction and discussion of two measures of performance, which are explored both analytically and experimentally.

Physical setup In order to empirically verify the improvement based on the models above, two test-bench physical setups are assembled, one for each actuator. Both actuators are controlled as described in Section 3.3.2 and using the same control gains. In this way, both systems can be approximated as in Equation 3.6 with the only difference being the inertia J_r. Gain values $P = 5$ and $D = 0.02$ are found empirically, gradually increasing P until slight oscillations appear and then adding a small D to sup-

	unit	Mk2	Mk1
Motor (Maxon)	-	EC60	EC90
Nominal supply voltage	V	24	36
Nominal power	W	100	90
Nominal torque	mNm	289	560
Nominal speed	rpm	3740	2510
Torque constant	Nm/A	0.053	0.109
Rotor inertia	$g \cdot cm^2$	1210	3060
HarmonicDrive	-	SHD-20-100-2SH	SHD-25-160-2SH
Reduction ratio	-	100	160
Torque sensor	-	ME-Systeme TS110a	
Parallel stiffness	Nm/rad	8	0

Table 3.1: Table summarizing the physical parameters of interest.

press them. The result is responsive torque tracking, with no instability observed during the tests. A commercial joint torque sensor (ME-Systeme TS110a, based on strain gauges) measures the interaction torque between actuator and environment. Its signal is amplified and acquired via custom electronics. A relatively low-stiffness parallel spring at $8Nm/rad$ is used in the PEA setup. At the moment of testing, this was the only spring available and was considered suitable to demonstrate the concept. This is a relatively low value, which would not enable Mk2 to generate $50Nm$ maximum torque in the target range of movements, which is approximately between 0 and $90deg = 1.57rad$ (see Fig. 2.4). With the cord used, the maximum portion of torque produced by the spring is approximately $12.5Nm$

at $90deg$. The experiments presented later in this chapter are adapted accordingly. However, on the implementation of the spring in [36] this value may be easily increased by employing thicker bungee cords.

3.4.1 Transparency

Transparency is a typical requirement for torque-controlled robots. It may be described as the actuator impedance perceived by the human when no assistance is required. In other words, a transparent exoskeleton should not interfere with user movements. A distinction is made here between *transparency* and *backdrivability*, another term used in this context. In fact, backdrivability is referred to as the mechanical reversibility of an actuator when unpowered rather than to a closed loop-controlled joint.

In the literature, different measures of transparency for exoskeleton joints have been used. One possibility is to observe the muscular activity across the human joint spanned by the exoskeleton. In comparison with moving with no exoskeleton, the lower the activity required to move the actuated joint in zero-torque mode, the more transparent that joint is considered [38]. Another, more direct measure is residual interaction force/torque, more commonly found in research studies [39, 40]. In this respect, low interaction forces/torques for the completion of the target movements are associated to more transparent devices. A drawback of these measures is that humans lack the ability to move in exactly repeatable trajectories, which makes comparisons across conditions difficult. The approach presented below has the advantage of being indipendent from precise repeatable trajectories, making it suitable to compare two actuators with different properties.

Considering the simplified joint dynamics in Equation (3.6) and ne-

glecting the less significant derivative term, transparency is quantified in terms of the reflected inertia in zero-torque mode, i.e. when $\tau_{ref} = 0$.

$$\tau_h \simeq \frac{J_r}{P+1}\ddot{\theta} \tag{3.8}$$

The lower the reflected inertia $\frac{J_r}{(P+1)}$, the lower the torques experienced at given accelerations and therefore the more transparent the actuator is considered in its interaction with the user. It is worth to note now that in this context the inertia J_r is what differs between actuators Mk1 and Mk2, as the P gain is set to the same value for both and has an upper bound associated to the stability limit (Section 3.3.2).

A factor F may be defined as:

$$F = \frac{J_{r,Mk1}}{J_{r,Mk2}} \simeq \frac{\tau_{h,Mk1}}{\tau_{h,Mk2}} \tag{3.9}$$

where $J_{r,Mk1}$ and $J_{r,Mk2}$ are computed as in Equation (3.5). The factor F captures the improvement in transparency from the old actuator to the newer, PEA-based implementation. Based on the physical parameters in Table 3.1, the expression in Equation (3.9) becomes

$$F = \frac{J_{r,Mk1}}{J_{r,Mk2}} \simeq \frac{J_{mg,Mk1} \cdot r_{Mk1}^2}{J_{mg,Mk2} \cdot r_{Mk2}^2} = \frac{3060 \cdot 160^2}{1210 \cdot 100^2} \simeq 6.5 \tag{3.10}$$

Experimental comparison In addition to the expression in Equation (3.10), an experiment was devised to estimate F from measured data. In this experiment, the two actuators are controlled in zero-torque mode with the same proportional and derivative control gains. Manual perturbations are applied via a link in a pseudo-sinusoidal motion spanning the joint velocities and accelerations of the target task. The measured interaction torques in the transparency experiment are shown in Fig. 3.4 against joint acceleration. The data show good fit to a linear relation between the two variables, which reflects the simplified dynamics in Equation (3.6). The ratio

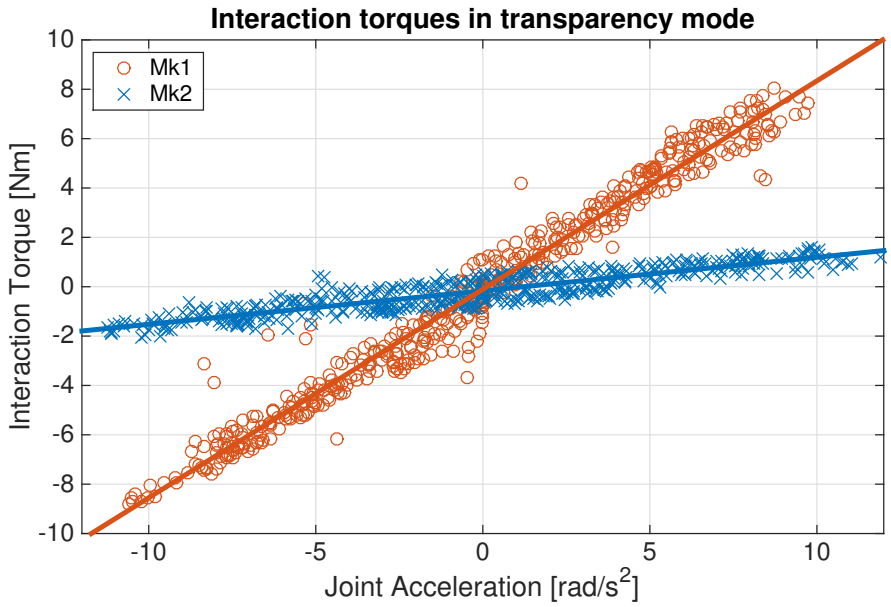

Figure 3.4: Interaction torques during transparency experiments plotted as a function of the acceleration. Red and blue lines are associated to Mk1 and Mk2, respectively.

between the slopes estimated for Mk1 and Mk2 thus represents the experimental estimation for the factor F in Equation (3.9). The slopes are computed using least square fitting, leading to

$$F^{exp} \simeq \frac{0.84}{0.13} \simeq 6.46 \tag{3.11}$$

which is just slightly lower than the prediction in Equation (3.10).

3.4.2 Dynamical accuracy

Dynamical accuracy is another relevant requirement for a torque-controlled system and is analyzed here in terms of achievable torque bandwidth

in controlled experimental conditions. For the sake of highlighting the torque dynamics of the actuators, its physical interaction with a simple elastic environment of stiffness k_e is considered such that:

$$\tau_h = k_e \theta_h \tag{3.12}$$

Considering the controller in Equations (3.2)-(3.3) applied to the system in Equation (3.1), neglecting the less significant terms, and using Equation (3.12), the following dynamics can be computed for the interaction torque τ_h

$$\frac{J_r}{k_e(P+1)}\ddot{\tau}_h + \frac{D}{P+1}\dot{\tau}_h + \tau_h = \tau_{ref} \tag{3.13}$$

This leads in Laplace domain to

$$\tau_h(s) = \frac{\omega_\tau^2}{s^2 + \frac{Dk_e}{J_r}s + \omega_\tau^2}\tau_{ref}(s). \tag{3.14}$$

where

$$\omega_\tau = \sqrt{\frac{k_e(P+1)}{J_r}} \tag{3.15}$$

Thus, the interaction torque follows the reference signal within a certain bandwidth that is proportional to ω_τ, which in turn depends on the reflected motor inertia. Estimating ω_τ would require the knowledge of k_e (see Equation 3.7 and associated paragraph for details) and is outside the scope of this study, which is limited to observing differences between two solutions acting on the same environment. Indeed, on a given environment, the improvement in dynamical performance may now be expressed in relative terms, with reference to Equation (3.15), as

$$\frac{\omega_{\tau,Mk2}}{\omega_{\tau,Mk1}} = \sqrt{\frac{J_{r,Mk1}}{J_{r,Mk2}}} = \sqrt{F} \tag{3.16}$$

where F is defined in Equation (3.9) and therefore

$$\sqrt{F} \simeq 2.5 \tag{3.17}$$

Experimental comparison An experiment is devised to support the analysis above. The physical setup includes the Mk1 and Mk2 actuators pressing on a coil spring. This is a very simplified representation of the human compliance at the physical interface, but it serves the purpose of comparing the performance of the two actuators. A dynamic torque-tracking task consists of a sinusoidal chirp signal as reference τ_{ref} with frequency gradually increasing to $6Hz$ over 30 seconds. The torque reference is asymmetric, i.e. offset to positive values to represent the asymmetry of torque range that is required by the exoskeleton. Namely, the reference signal is built of a $10Nm$ offset and a moderate $2Nm$ amplitude, chosen empirically to avoid unmodelled saturation phenomena in the motor drives. The experimental data is then used to identify the parameters of the transfer function from τ_{ref} to τ_h in the frequency domain, assuming no zeros and two poles as in Equation (3.14). The ARMAX algorithm within the Matlab Identification Toolbox is used for the identification with τ_{ref} and τ_h as input and output signals, respectively. The results of this experiment are shown in Fig. 3.5 in terms of pole location and Bode plots, respectively. The dynamics of the two actuators shows a large difference in the frequencies at which their poles are located. Mk1 is identified as characterized by a frequency of $12.5rad/s$ $(2Hz)$, whereas the poles of Mk2 have a frequency of $30.5rad/s$ $(4.85Hz)$ leading to

$$(\sqrt{F})^{exp} = \frac{\omega^{exp}_{\tau,Mk2}}{\omega^{exp}_{\tau,Mk1}} \simeq \frac{30.5}{12.5} = 2.44 \tag{3.18}$$

which is slightly lower than predicted in Equation (3.17).

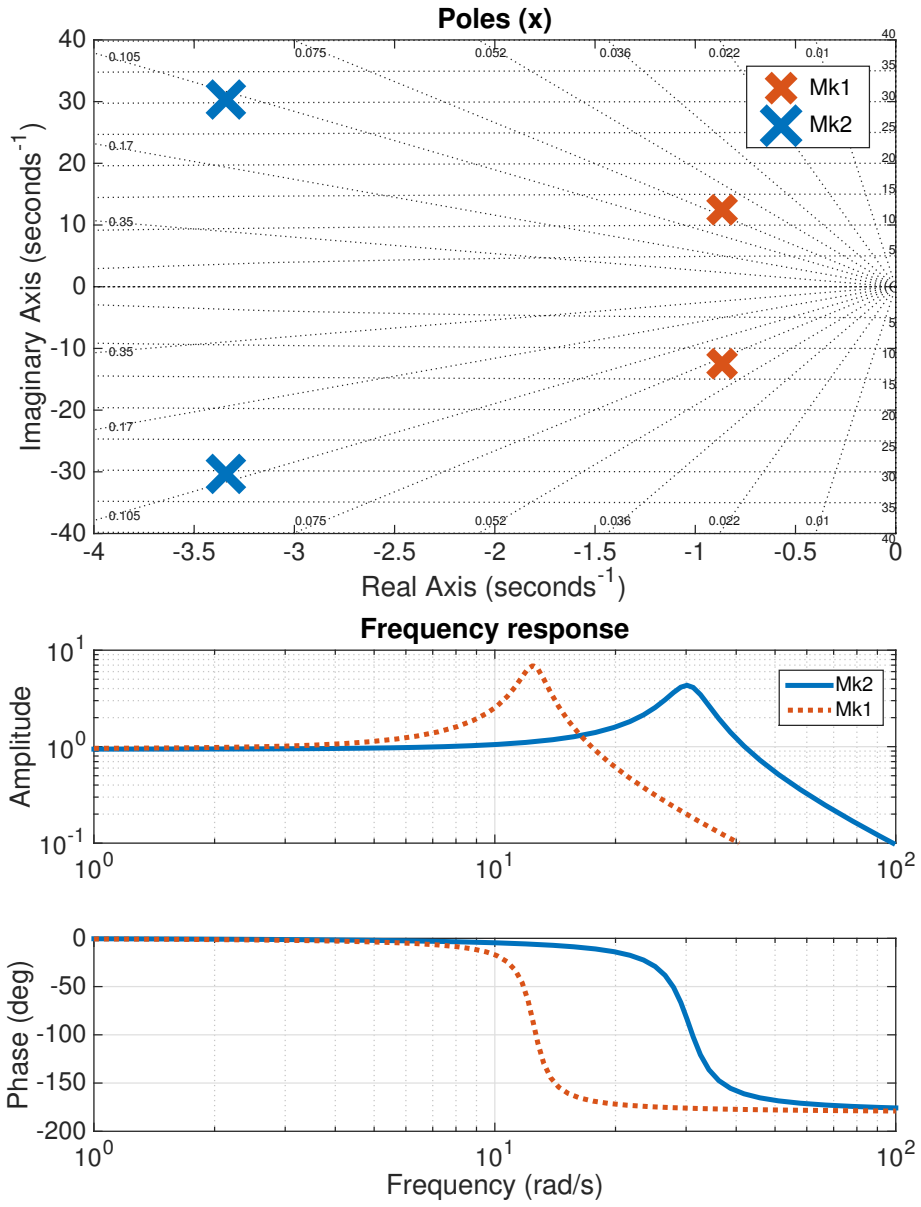

Figure 3.5: Pole locations and frequency responses from τ_{ref} to τ_h when the actuator is coupled to a physical spring. The red and blue lines correspond to Mk1 and Mk2, respectively.

3.5 Discussion

Prior work on elastic robotic actuators has focused mostly on their power and energy consumption in cyclic tasks [27, 41]. Comprehensive models of energy losses have been used to suggest design solutions including series and parallel elasticity [32].

In the force control literature, SEAs are a common choice leading to improved force-control robustness via reduced output stiffness [35]. Considering the requirements for soft physical interfaces in wearable robots, the inherent human compliance (and the additional exoskeleton compliance) may reduce the need for series elasticity at the actuator.

Parallel elastic elements have been shown to reduce motor torque requirements for joints subject to substantial static loads [28, 31, 34]. The present research borrows this consideration and focuses on torque-control dynamics, which in the area of wearable exoskeletons is perceived as more impactful to maximize user experience. The present study starts from the joint torque requirements and proposes a rationale to choose a PEA, based on a convenient choice of motor. The formulation in Section 3.3 and the observations in Section 3.4 suggest substantial improvement in the proposed measures of torque-control performance associated to lower-inertia actuators. Important limitations of this study are connected to the assumptions made to obtain the simple measures of torque dynamics proposed. These measures should in fact be considered as an immediate tool to compare actuators with different inertias, acting under given implementation constraints associated to the physical interaction with the environment.

Weight and cost are additional aspects related to the implementation of the parallel spring that are not considered in this study. Indeed, the current

custom implementation of Mk2 is heavier and more expensive than Mk1, which by contrast is mostly made with commercially available components. The present study represents a first step in showing the advantages of parallel-elastic actuation for exoskeleton joints, while further engineering work on the associated hardware is planned for subsequent stages.

4 Control strategies

Summary Active exoskeletons have the flexibility of implementing physical assistance for different tasks and adjusting to different users and conditions. Assistive strategies represent the key to exploiting this flexibility. This is currently an open challenge towards commercially successful devices outside laboratory settings. The challenge mainly lies in the compromise between minimally obtrusive, cost-effective hardware and extracting meaningful information on user intent resulting in intuitive use. This chapter presents the implementation of different assistive strategies exploiting combinations of user posture and muscular activity to modulate the assistive forces generated by the exoskeleton. The advantages lie in the unobtrusive implementation and strong versatility.

Parts of this chapter have been submitted for publication as: **Toxiri, S.**, Koopman, A. S., Lazzaroni, M., Ortiz, J., Power, V., de Looze, M. P., O'Sullivan, L., & Caldwell, D. G. Rationale, Implementation and Evaluation of Assistive Strategies for an Active Back-Support Exoskeleton. *Frontiers in Robotics and AI*.

4.1 Introduction

Passive exoskeletons tend to be simple and lightweight. However, because they only generate forces via mechanical springs, they lack flexibility as their action cannot be automatically adjusted to different users or conditions. For example, a passive device does not modulate the support it provides based on the load being lifted, and it is typically designed for very specific tasks. By contrast, robotic actuators offer intrinsic versatility but conversely increase the complexity, weight, and cost of exoskeletons.

The key to versatility and therefore a crucial component in the success of active exoskeletons is a suitable assistive control strategy. Assistive strategies consist of the sensors and associated computer programs that modulate in real time the power provided by the actuators at the corresponding human joints. In practical terms, the problem they address is to generate appropriate reference signals to control the speed, torque or impedance of the actuated joints over time. This aspect remains an open challenge due to the difficulty in acquiring meaningful information on user intent [42, 43, 44, 45].

Possible ways to infer user intent and needs strongly depend on the target task. Every strategy has different advantages and drawbacks associated to the obtrusiveness of the sensors it uses and the active user participation it requires. In order to assist walking, for example, it might be practical for a lower-limb exoskeleton to exploit the periodicity of the task and play joint trajectory profiles in loops. In this case, no obtrusive sensor would be necessary outside the main structure of the exoskeleton. However, while little user participation would be required, a possible drawback is that the user would have no influence on the assistance.

The task of interest in the present work is manual material handling in industrial applications, i.e. human operators repeatedly lifting, carrying and lowering heavy objects. Not only is this task not periodic, it is also associated to greater variability as the mass of the external object is unknown a priori but has strong influence on the torques necessary to accomplish the task. As a result, it is of particular importance to find an appropriate method for capturing user intent to appropriately command an assistive device. This work is an attempt to exploit the advantage of actuated devices by exploring control strategies for an active, torque-controlled back-support exoskeleton. The specific problem addressed here is modulating the magnitude of the assistive torque that the exoskeleton should produce on its user over time to make a meaningful and substantial contribution. In other words, the above can be expressed as generating a continuous reference torque that the exoskeleton actuators should track. To this end, the combination of user posture and muscular activity to generate reference assistive torque are explored. The proposed methods are very little obtrusive and result in intuitive interaction between the exoskeleton and its user during the target task.

This chapter describes the implementation of a number of different assistive strategies and discusses their advantages and drawbacks. Firstly, a critical overview on the relevant state of the art is presented. A brief description of the overall control scheme for the back-support exoskeleton is provided in order to focus the attention on the problem addressed in this chapter. The remaining part describes the implementation and preliminary evaluation of the different assistive strategies, discussing their relevance to the target task.

4.1.1 Prior work

While actuation technology is similar across many exoskeletons, a wide variety of control strategies can be found in literature. As the strategy largely determines the assistive action provided by an exoskeleton to its wearer, it typically needs to be designed for the specific target task. A number of reviews on control strategies have been published in recent years [44, 45, 46, 47, 48, 49]. Although their focus is mostly on lower-limb exoskeletons to retrain or assist walking, there are a number of concepts that it is helpful to borrow. For example, it has become common to distinguish between *direct* and *indirect* strategies, depending on whether information is acquired from the user (e.g. biosignals) or from the environment (e.g. joints motion or ground reaction force), respectively.

Indirect strategies

Commanding an exoskeleton based on the motion of relevant body segments is particularly suited to cyclic tasks such as walking. In this case, an exoskeleton would attempt to match the cadence and reproduce a set of predefined assistive actions in loops. Relevant examples are presented in [50, 51, 52] with applications in elbow and hip assistance. It is helpful to highlight here that sensors for joints orientation are usually well integrated in the exoskeleton and are therefore little obtrusive. Also, measurements of interaction forces have been used as inputs for assistive strategies. Ground reaction force (GRF) is used in combination with knee joint angle on the RoboKnee to provide assistance against gravity [53]. A similar approach is taken on a different and somewhat unique device, the Honda Walking Assist Device [54]. With focus on lifting objects rather

than walking, GRF is used to generate commands for a wearable knee exoskeleton [55] and for a ground-based robotic arm [56]. One of the issues typically associated to these measurements is the obtrusiveness of the sensors that measure the GRF. In some cases they may limit movement, in others they may require being worn inside the user's or special shoes. In industrial applications, where users are not intrinsically motivated to wear assistive device, these limitations may compromise their acceptance. BLEEX is a well-known lower-limb exoskeleton for performance augmentation in walking long distances with heavy loads [57]. The idea is that the load is part of a backpack and its weight redirected to the ground via the exoskeleton structures. The actuated joints, strapped onto the user's leg segments, are commanded to follow the user movements with the lowest interaction forces possible. This is indeed the key feature of this strategy, which makes it unsuitable for devices designed to apply substantial assistive forces onto the user to reduce loads on specific parts, as is the case in this thesis. The latter is also the case with the HAL Lumbar Support, which is of the same class as the device used in this thesis [24]. One of its control modes is based on a well-integrated measure of posture. Assistance is then provided as a force proportional to the inclination of the torso. This is of particular interest in the present chapter.

Direct strategies

Electromyography (EMG) is perhaps the most representative technique for direct control of exoskeletons[1]. This technique is based on measur-

[1]Electroencefalography (EEG), aimed at measuring brain electrical activity as reflected on the surface of the scalp, is a comparatively more invasive technique, at this stage still more suited for use in the laboratory. It is thus not considered in this work.

ing very small electrical signals that are directly associated to muscular activity. While invasive implanted electrodes exist (especially in medical applications), the focus here is only on non-invasive surface electrodes that capture muscular activity as reflected on the corresponding skin surface. Electromyography is a relatively complex technique, which has historically been used in many different applications in the laboratory and suffers from some practical limitations. Applications for monitoring purposes are not of interest here (see [58, 59] for a complete overview), thus it is considered most helpful to first outline its uses for controlling exoskeletons, while practical limitations are discussed in a dedicated paragraph below.

A major trend in the literature is to employ a model to map the measured muscular activity into exerted muscle force and command an exoskeleton accordingly, e.g. regulating the speed or force at its joints. Some examples can be found in [60, 61, 62]. Using similar models, Karavas and colleagues estimated human joint stiffness by reading the activity of two antagonistic muscule groups at the knee [63]. In that study, the mechanical stiffness displayed by a knee exoskeleton was controlled correspondingly. A central component of these approaches is the use of a model of muscular force, for which the identification of a number of parameters is typically required.

In contrast with previous literature supporting the need for accurate models, recent studies have successfully implemented more straightforward approaches whereby EMG amplitude is more directly and proportionally mapped into a reference force/torque for an exoskeleton joint. A study on the HAL Lumbar Support tested this *proportional myoelectric control* [24] (which will be discussed further in this chapter). Lenzi *et al* later

highlighted its relevance, proposing that an approximate measure of muscular activity may indeed be sufficient to control assistive exoskeletons [64]. An additional study by the same group successfully showed that a device assisting one joint may even be controlled via a muscle acting on a different joint, as long as the two muscle groups are activated in coordination during the target task [65]. These findings encourage further research towards the simplification of direct control strategies for wearable robots, thus making their adoption more likely and impactful on the wide public. Recent applications of proportional myoelectric control are also described in [66, 67]. In addition to electromyography, a number of younger technologies have been adopted but are not considered mature enough for industrial applications [68, 69].

Practical limitations of EMG interfaces The successful application of EMG for control purposes has historically been limited due to a number of practical shortcomings. Firstly, the physical attachment of electrodes often requires careful skin preparation and electrode placement to improve the quality and content of the signal. The signal is also subject to artifacts associated to sweat, muscle fatigue and involuntary impacts. Additionally, in association to relatively complex models of muscular force, relatively time-consuming calibration procedures are necessary and specific to subjects and individual sessions. These practical issues make traditional EMG-acquisition setups unsuitable for industrial applications, for which quicker and simpler solutions would be more appropriate. In this respect, the solution proposed in this study and described in the next section represents a substantial improvement.

4.2 Proposed strategies

Two-level scheme The overall control scheme of the back-support exoskeleton is structured on two levels, as illustrated in Figure 4.1. The low level regulates the torque output at each actuator via a closed-loop proportional-derivative controller (as described in Chapter 3). The high-level controller corresponds to the assistive strategy and is of central importance in this study. The high-level strategy is responsible for generating the torque reference signal that is tracked by each actuator. The general goal of this scheme is that user should be free to move as intended and should additionally experience substantial assistive forces, modulated with appropriate timing and extent. This concept has been referred to as *following user intention*.

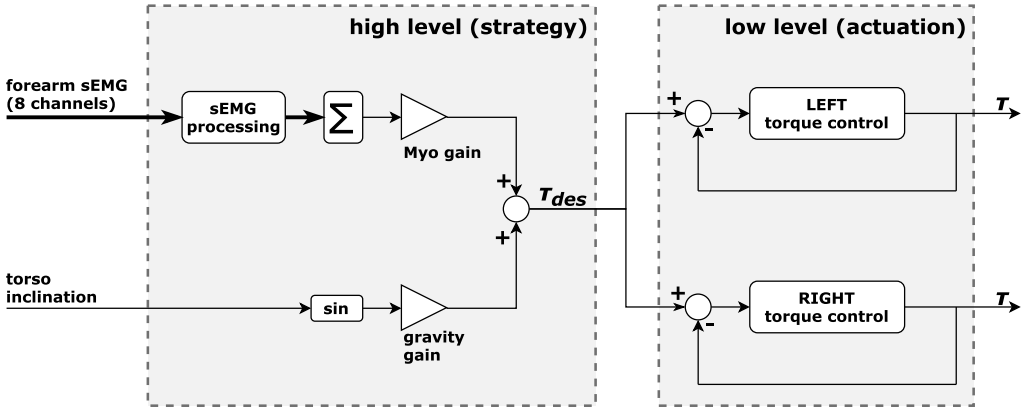

Figure 4.1: The implemented control scheme, articulated in two levels. The low level regulates the torque output at the actuators. The high level, composed of two parallel branches, corresponds to the assistive strategy and is responsible for modulating the extent and timing of the generated assistance.

Rationale A simplified two-dimensional model is employed to gain quantitative understanding of the biomechanics of the lumbar spine during the target task. The model, illustrated in Fig. 2.1 and detailed in [26], represents the lumbar spine as a rotational joint connecting the torso mass W_T to the pelvis, which is simplified as attached to ground. The spinal muscles, responsible for back extension, are represented as generating a force F_M parallel to and posterior to the spine (at a d_M distance). The reaction force R_C at the joint captures the lumbar compressive loads, which the exoskeleton aims to reduce. The external object is represented by an additional (variable) mass W_L, rigidly connected to the upper body. Human motion data[2] applied to this model allows the estimation of the net lumbar moment via inverse dynamics (Fig. 4.2, on the left). This estimate is then used to compute the corresponding muscular force (Fig. 4.2, center) based on an approximated, fixed lever arm. Fig. 4.2, on the right, shows the estimate of the resulting compressive force acting on the lumbar spine while handling objects from $0kg$ to $15kg$.

Two key factors appear to affect lumbar moment, muscular force and lumbar compression in the same way: (a) the *orientation of the upper body*, and (b) the *mass of the object* being handled. The compression increases with the orientation angle, reflecting a corresponding increase in muscular activity. Indeed, greater forces at the *erector spinae* muscle group are necessary to balance the moment generated by gravity acting on the users upper body and external mass. As a consequence, greater compression is associated to increasing object mass. Similarly to above, the spinal muscles activate to balance the increasing load and in turn larger compressive

[2]Thanks to the Netherlands Organisation for Applied Scientific Research (TNO) for providing the data.

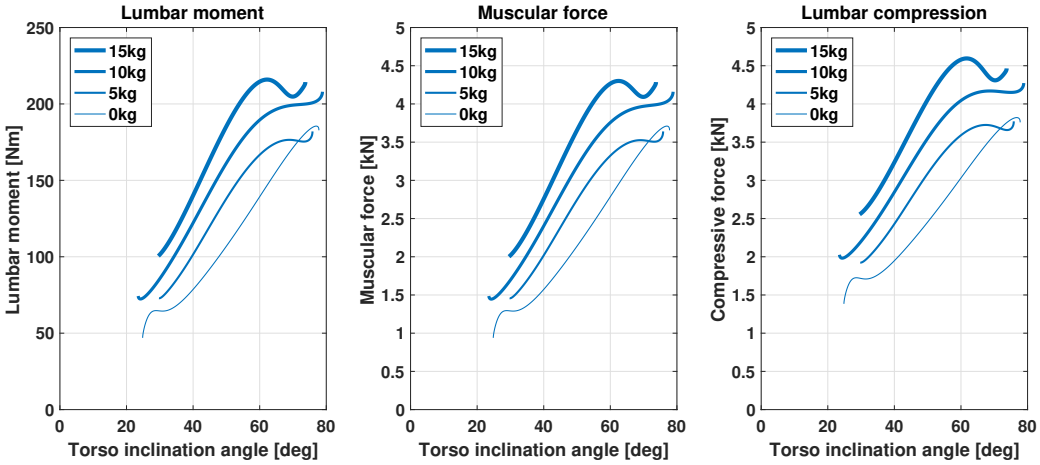

Figure 4.2: Lumbar moment (left) computed via inverse dynamics, applying real motion data to the model in Fig. 2.1. As a consequence, the muscular force F_M (center) and joint reaction force R_C (right) are calculated. The three show similar trends, depending on two key factors: (a) the *orientation of the upper body*, and (b) the *mass of the object* being handled.

reaction forces are generated on the lumbar joint.

In order to promote appropriately timed and modulated physical assistance based on the considerations, the two factors were taken into account for the design of the assistive strategy for the exoskeleton. Fig 4.3 provides a qualitative illustration of the strategies. The stick figures at the top represent the key movements target task: a person, starting in an upright posture, bend down to pick up a box and stands back up while holding it. The person then bends down again to set the box back to its original position. The strategy in red (Section 4.2.1) commands for assistance when the person is bent down, independently of where the box is. By contrast, the strategy in blue switches on when the box is held. As described in

Section 4.2.2, this strategy is additionally designed to increase assistance corresponding to heavier boxes. The yellow line represents a third, more general, strategy which is a combination of the two above (Section 4.2.3).

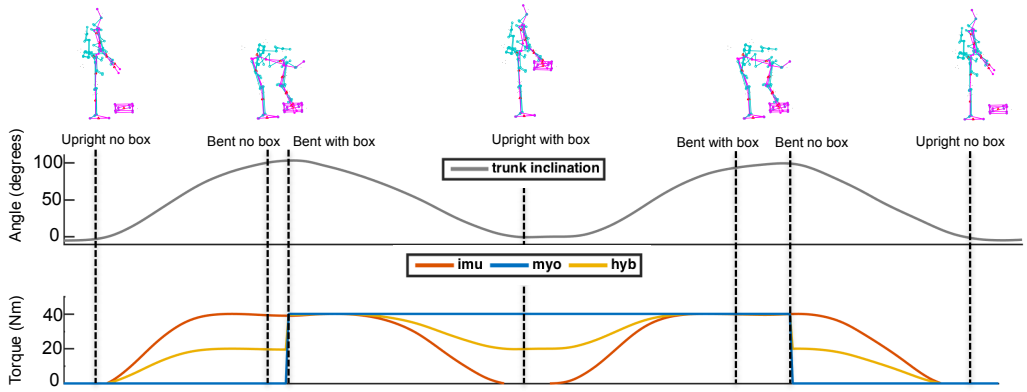

Figure 4.3: This simplified illustration further describes the idea behind the implemented control strategies. In red, *imu* follows the inclination of the torso regardless of whether the user is holding the object. The *myo* mode (blue line) is represented as only switching on when the user holds the object. In yellow, *hyb* displays a combination of the two behaviors, in which each branch contributes to half of the generated reference torque.

4.2.1 Inclination-based

One branch implements an approximate version of what on a robotic arm would be known as *gravity compensation*. The idea is to relieve the user from the effort spent on holding the torso link of the exoskeleton as well as his/her own torso. The implementation does not attempt to precisely estimate the mass properties of the users upper body and exoskeleton links to exactly cancel the effects of gravity. Rather, the gain corresponding to

this branch is adjusted individually during a preliminary familiarization session, based on the users own comfort and/or preference.

$$\tau_{des} = K_{imu} \cdot sin(\theta_{trunk}) \tag{4.1}$$

Note that this implementation differs from the model in Section 2.1.2 and Equation 2.5, which represents a hypothetical physical spring. The torso inclination angle is acquired via an xSens MTi-30 AHRS inertial measurement unit (IMU), solidly attached to the exoskeleton back structure.

4.2.2 Proportional myocontrol

The second, sEMG-based branch is at the core of the proposed assistive strategy. Typically, the activity of one or more muscles acting on the assisted joint would be acquired, so that the same physical activity can be accomplished with less muscular activity. Examples from recent literature are [66], in which the activity of gluteus and quadriceps was used to modulate assistance at the hip, and [67], in which elbow flexion is assisted with forces modulated on biceps activity. The closest example to the present work is reported in [24]. In that study, HAL Lumbar Support assisted hip and back extension proportionally to the activity of the spinal muscles. By contrast, the controller presented here generates reference values for the assistive torques proportionally to the activation of the forearm muscles, which act in coordination with the spinal muscles when manually lifting objects. As anticipated earlier in this chapter, the concept of assisting a muscle based on the activity of a different one was first explicitly described in [65]. This option is suitable if during a given task, the two muscle groups activate in coordination (see section below),

and if measuring the activity of the main muscle is technically challenging in practice while the secondary muscle is more easily accessed.

The activity of the forearm muscles is recorded by the electrodes on the Myo armband (a description of this device is provided in a section below). As opposed to the activity of any specific muscle at the forearm, their overall activity is considered. Thus, the sum of the eight rectified signals acquired was considered as an estimate of grip strength, and therefore chosen to represent the intention of the user. The signal generated at this stage is loosely referred to as *myo*. It is normalized during a quick calibration phase aimed at measuring the value it reaches at maximum muscle contraction. The control scheme generates the corresponding component of the assistive torque as proportional to the normalized *myo* signal, via a gain that determines to what extent the exoskeleton contributes to the task, and thus potentially reduces the users effort to accomplish it.

$$\tau_{des} = K_{myo} \cdot EMG_{sum,norm} \tag{4.2}$$

4.2.3 Hybrid

The more general case of the strategy illustrated in Fig. 4.1 is referred to as *hybrid* strategy. In this general case, the two inclination-based and EMG-based branches are active at the same time, each of the two regulated by the corresponding control gain, as follows:

$$\tau_{des} = K_{imu} \cdot sin(\theta_{trunk}) + K_{myo} \cdot EMG_{sum,norm} \tag{4.3}$$

In principle, it is possible to adjust K_{imu} and K_{myo} for each user and/or tasks to best meet personal preferences and task conditions.

Figure 4.4: The Myo armband.

The Myo armband As part of our approach, muscular activity at the forearm is measured via an inexpensive commercial device based on surface electromyography. The Myo gesture control armband[3] (shown in Fig. 4.4) offers eight pairs of dry electrodes, equally spaced around the band, typically worn on the forearm. This device is convenient for a number of reasons, besides its affordability. The surface electromyography on the Myo uses dry electrodes. This solution requires no skin preparation nor pre-gelled disposable electrodes. Considering the target task of lifting object, wearing a compact armband is less invasive than the corresponding setup on the low back underneath the clothes. In fact, this would require an additional person for the skin preparation and electrode positioning, besides potentially limiting the user's movement and resulting in poor signal quality due to mechanical interference with the exoskeleton struc-

[3]http://www.myo.com

ture and/or straps. As an additional benefit, the device sends out data via a practical wireless communication and is powered by built-in batteries. The following section provides the details of how the signals acquired by the Myo armband are used to command the exoskeleton. The sEMG signals acquired on the forearm were preprocessed on the Myo armband itself. A custom script received the eight filtered and rectified signals and made them available to the main program controlling the exoskeleton. For the purpose of control, the signals were summed and further low-pass filtered with a cut-off frequency set to $3Hz$, chosen empirically as a trade-off between physical comfort and responsiveness.

4.3 Discussion

The ability to implement different strategies is the central advantage of active exoskeletons. Associated to this ability is the potential to adapt immediately to different users and task conditions, which provides superior versatility in comparison to passive systems. As the field tends towards designing assistive devices with high specificity to one task, it is conceivable to address multiple tasks with one, appropriately adaptable, active exoskeleton as opposed to many specific passive ones. Practically, the above means that the same exoskeleton may readily adapt to different tasks wherein one or the other branch may be more or less necessary. For example, in a factory, the exoskeleton may be used to assist multiple, potentially different, tasks by selecting an appropriate strategy from an available set, and/or further adjusting the parameters of each based on specific needs. While switching between strategies could easily be offered as a voluntary option to the user, it is also conceivable to automatically

and online recognize the activity based on a set of relevant measurements [70].

By design, the *imu* and *myo* strategies are each meant to address one of the factors affecting lumbar compression and thus need for assistance. Also, each is associated to advantages and drawbacks that need to be considered in the context of use of the exoskeleton. The *imu* strategy has the advantage of only relying on very well integrated hardware, entirely external to the user. The disadvantages are connected to its inability to modulate the assistance to varying loads. Therefore, it may be a good solution by itself when the load is known in advance, or for the specific case of supporting static postures. By contrast, the capability of the EMG-based component to maintain substantial assistance whenever the user holds an object (and proportionally to its mass) is considered a beneficial feature for an exoskeleton designed for repeated lifting. An additional difference is connected to the possibility of scaling the assistive forces up. As mentioned, the *imu* strategy is suited for known loads. The (known) value of the load may for example be used to scale the assistance up or down by adjusting the corresponding gain K_{imu}. However, larger gain would lead to increasing forces also when no object is being held and thus no (or only low) assistance is necessary, generating unwanted hindrance. Conversely, larger *myo* gains K_{myo} would lead to greater forces corresponding to heavier loads, therefore according to an increased need for assistance. This aspect makes this strategy of particular interest considering the possible future development of actuators, capable of generating larger forces at the required speeds. Based on the above, the *hybrid* strategy potentially combines the advantages and carries the drawbacks of the two strategies above.

It is important to highlight that the advantage discussed above relies on the physical effectiveness of each of the strategies implemented on an exoskeleton. The biomechanical beneficial effect of an exoskeleton and specific strategies needs to be validated by dedicated studies. While this aspect is outside the scope of a thesis focused on advancing the enabling technologies, no exoskeleton research and development is complete without producing convincing evidence that its physical effects are as originally intended. The following chapter covers the methods that have been employed to validate the prototypes and concepts described until this point.

5 VALIDATION

Summary The testing and subsequent adoption of exoskeletons in the workplace is encouraged first of all by evidence of their physical effectiveness. To this end, this chapter complements the core contributions of this thesis by describing the methods for validation and some results of the experimental campaigns carried out on the prototype.

Reduction in relevant muscle activity represents a non-invasive, convenient way of directly measuring the effect of an exoskeleton during a physical task. A more complete approach includes more time-consuming laboratory procedures aimed at estimating the actual compressive forces on the target joints. The results of the experimental campaign are in line with the literature on comparable devices and provide encouraging evidence on the effectiveness of the prototype presented.

Parts of this chapter have been submitted for publication as: **Toxiri, S.**, Koopman, A. S., Lazzaroni, M., Ortiz, J., Power, V., de Looze, M. P., O'Sullivan, L., & Caldwell, D. G. Rationale, Implementation and Evaluation of Assistive Strategies for an Active Back-Support Exoskeleton. *Frontiers in Robotics and AI*.

5.1 Introduction

This chapter provides an overview of the methods for the validation of the prototype exoskeleton, presents results of interest and discusses their relevance. For an exoskeleton to be successfully adopted in the field as a product, there are two crucial components of validation. On the one hand, its effect on the user's body must be as originally intended. Depending on the specific case, this may translate into lower metabolic cost or muscular activity, reduced joint loading, etc. On the other hand, the device must be accepted well by users, who feel encouraged to use it, and must be affordable and integrate well with the existing infrastructure, so that employers are motivated to purchase it. It may be reasonably argued that the first component is preliminary to the second one. In other words, employers and workers will only be willing to test a device in the field once convincing evidence of its beneficial effects on the human body is available.

As it emerges from the review by de Looze *et al* [4], the majority of studies reporting the effects of exoskeletons focus on reductions in muscular activity. This is often a case of convenience, as muscular activity can be quite readily measured with non-invasive laboratory technologies (although not free of complications). On the other hand, joint loading can only be estimated indirectly[1] and requires the use of additional technology (e.g. motion capture setups) and musculoskeletal models, which results in substantially more time-consuming testing procedures. In relation to the lumbar spine, muscular activity is considered a reliable indicator of joint loading, as described in Section 2.1. Therefore, a significant reduction in

[1]Instrumented implants for in-vivo measurement exist, but are rather invasive and therefore not considered here.

muscular activity at the spine is reasonably associated to an improvement in the corresponding compressive loads. In combination with reduced activity at the target joint, an exoskeleton should not increase the activity or loading on different joints to the point where these are at significant risk of injury. For example, a common concern with back-support exoskeletons is that the loads may be transfered to the knees to an excessive extent.

Experiments to validate the physical effectiveness of exoskeletons are often performed in controlled laboratory settings. For back-support exoskeletons, the tasks typically involve some type of static and dynamic lifting meant to represent the activities carried out in the workplace. As the objective is to capture the effect of the exoskeleton, the most central independent variable reflects whether the task is peformed with or without the assistance of the device. Another important variable that applies to active exoskeletons is the strategy by which they are controlled, when more than one is available (as is the case in the experiments presented here). Additional conditions may consider different loads and lifting techniques (i.e. squat or stoop).

5.2 Methods

A recent testing campaign was performed on a refined version (Mk2b) of the prototype described in Section 2.3. Besides refined electronics and software, the main difference is the absence of the parallel spring described in Chapter 3. This decision was made to maximize compactness, although at the cost of reduced torque capabilities. The experiment attempted to replicate the scenario of the target task, with the goal of observing differences between the different strategies described above. The tests took place in

October 2017 at the Vrije Universiteit Amsterdam and involved 11 participants[2]. The exoskeleton was controlled based on three different strategies: inclination-based using $K_{imu} = 20$ (Section 4.2.1); myocontrol-based using $K_{myo} = 20$ (Section 4.2.2); a hybrid of these two using $K_{imu} = 10$ and $K_{myo} = 10$ (Section 4.2.3). The activity of *erector spinae* muscles (specifically, the *iliocostalis*) was acquired on both the left and right side using a portable EMG system. Skin preparation and signal processing (filtering, rectification and normalization) followed SENIAM procedures [71].

5.2.1 Experimental task

Each subject was instructed to complete a lifting and lowering task in different conditions, described as follows:

- *no exo*: no exoskeleton is worn;
- *imu*: the exoskeleton assists based on the inclination strategy (Section 4.2.1), with $K_{imu} = 20$;
- *myo*: the exoskeleton assists based on the sEMG strategy (Section 4.2.2), with $K_{myo} = 20$;
- *hyb*: the exoskeleton assists based on the hybrid strategy (Section 4.2.3), with $K_{imu} = K_{myo} = 10$.

The first condition was performed first in all cases, while the order of the remaining three was randomized. As part of the task, each condition started in an upright position (Fig. 4.3 provides a helpful illustration). The

[2]This study was carried out in accordance with the recommendations of The Scientific and Ethical Review Board (VCWE) of the Faculty of Behavior & Movement Sciences, VU University Amsterdam (VCWE-2017-138).

participant would then bend over, reach and grasp an object from mid-shin height and take it up to an upright position. With no interruption, the participant would then bend over once more, place the object back into its original position, go back to an upright posture, and repeat this procedure for a total of three repetitions. This segment was executed twice, starting with a $7.5kg$ object and then with a $15kg$ object, so that for each condition the participant would lift and lower a total of six times. No instructions on a specific lifting technique (i.e. stoop or squat) were given to the participants. The object consisted of a container with handles, loaded with known weights that could be removed to accomodate for the different loads during the experiment. For the purpose of calibrating the corresponding control strategy, the *myo* (forearm) sEMG signal was normalized for each participant during a preliminary calibration session, during which a $15kg$ object was held for one second against gravity.

5.2.2 Data analysis

The sEMG signals were rectified and filtered according to standard practice (low-pass frequency at $2.5Hz$), and ultimately normalized to the maximal voluntary contraction (M.V.C.) acquired during a preliminary procedure. For each condition and object mass the peak activity was considered, ultimately using the average value between left and right side.

5.3 Results

5.3.1 Reference torque profiles

It is interesting to observe how the torque reference generated by each of the three strategies differs in terms of timing and extent of the assistance provided to the user. For illustration purposes, data from one subject is shown in Fig. 5.1. The total reference torque is plotted together with the corresponding signal for torso inclination, to relate with the movement of the user.

In the first row, the red profile associated to the *imu* strategy produces a reference that mostly overlaps with the torso orientation both on the left and the right plot, corresponding to the $7.5kg$ and $15kg$ object respectively. In the second row, the blue signal represents the reference generated by the *myo* strategy. The reference torque increases corresponding to when the user picks up the box (left peak in torso inclination angle), and decreases again when the box is released (right peak in torso inclination angle). Additionally, generally larger torques are generated corresponding to the heavier object (right column). The third row shows intermediate trends between the two above. The yellow reference torques follow the orientation closely, although their values in between peak pairs are larger for the heavier object.

5.3.2 Muscular activity

The results for muscular activity are shown in Fig. 5.2. At the top, the activity profiles are shown as averaged across all subjects, together with the corresponding profiles of torso orientation (dashed lines). With respect to

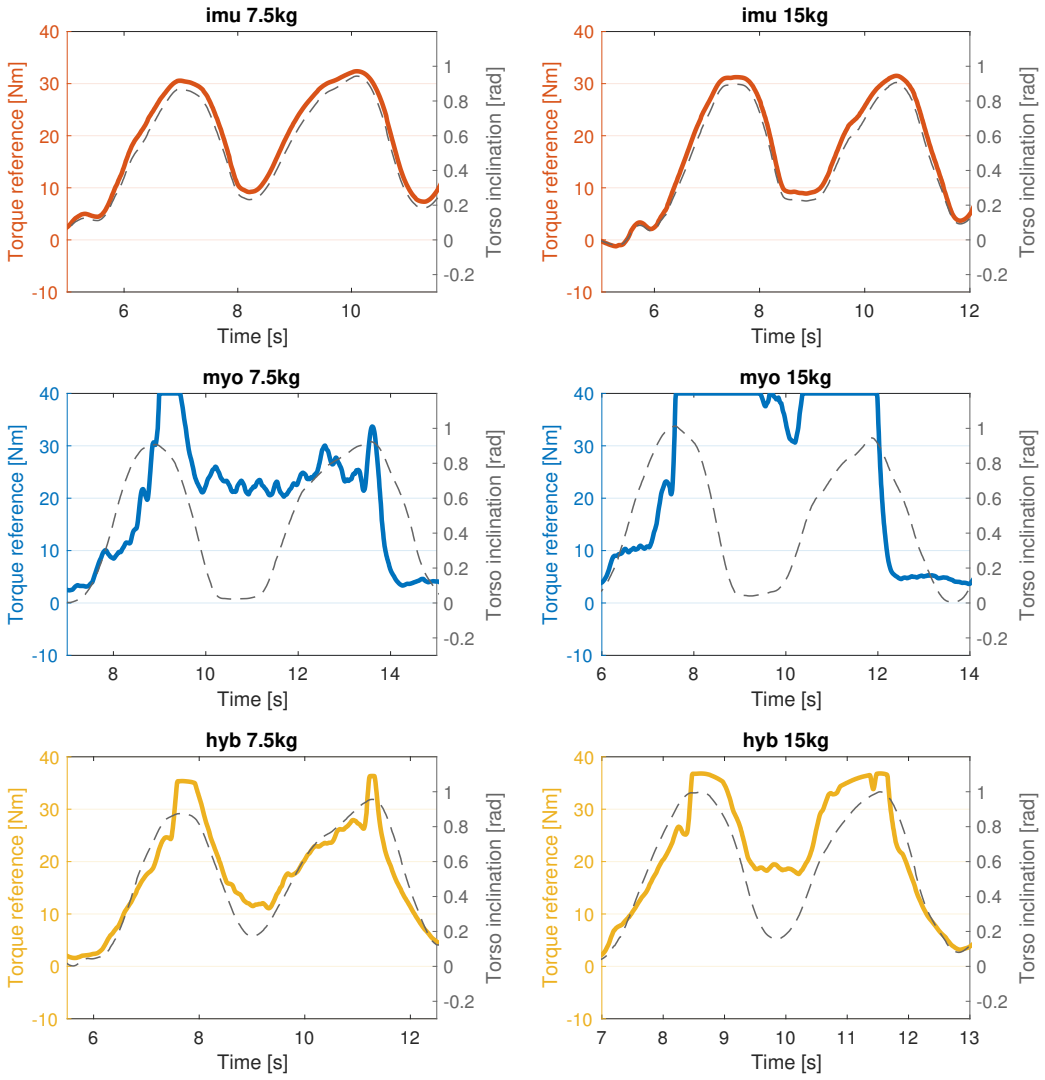

Figure 5.1: Torque reference profiles generated by each of the three strategies. Data is shown for illustration purposes, for one subject. The red signal mostly overlaps with the torso orientation, while the blue lines in the second row is high between the peaks, and the value is larger for heavier load (on the right). In the third row, the *hyb* reference displays an intermediate behavior between the two above.

the *no exo* (green) condition, reduced activation of the spinal muscles is observed in all cases. More in detail, the average profile associated to the *imu* (red) control leads to the lowest activation during the first phase (before $2.0s$), before the user reaches the object. The same holds for the final phase (around $6.0s$), when the person is standing back up after releasing the object. This consideration is valid for both loads: $7.5kg$ (left plot) and $15kg$ (right plot). By contrast, *myo* (blue) is associated to lowest muscular activity in the phase (around $3.5s$). This time corresponds to the second descent phase when the user is holding the object and, from an upright position, bends forward again to take the box back down. At the same key times, the yellow profile representing the *hyb* condition displays intermediate values with respect to the two above.

The bottom part of Fig. 5.2 shows the activity peaks averaged across all subjects for the different conditions. Similarly to average activation profiles, peak activation is also reduced by all three strategies, for both loads. With respect to the *no exo* condition, significant percentage reductions ($p < 0.05$) in the peaks ranging from 28% to 35% were observed.

5.4 Discussion

The results indicate that the use of the exoskeleton, controlled by any of the proposed strategies, leads to reduced activation of the spinal muscles. This is positively associated to reduced compression forces at the lumbar spine and therefore suggests potentially lower risk of musculoskeletal injuries during repeated lifting activities. The numbers found in this study (percentage reductions between 28% and 35%) are in line with those indicated in the existing literature (see [4, 9]), which confirms the effectiveness

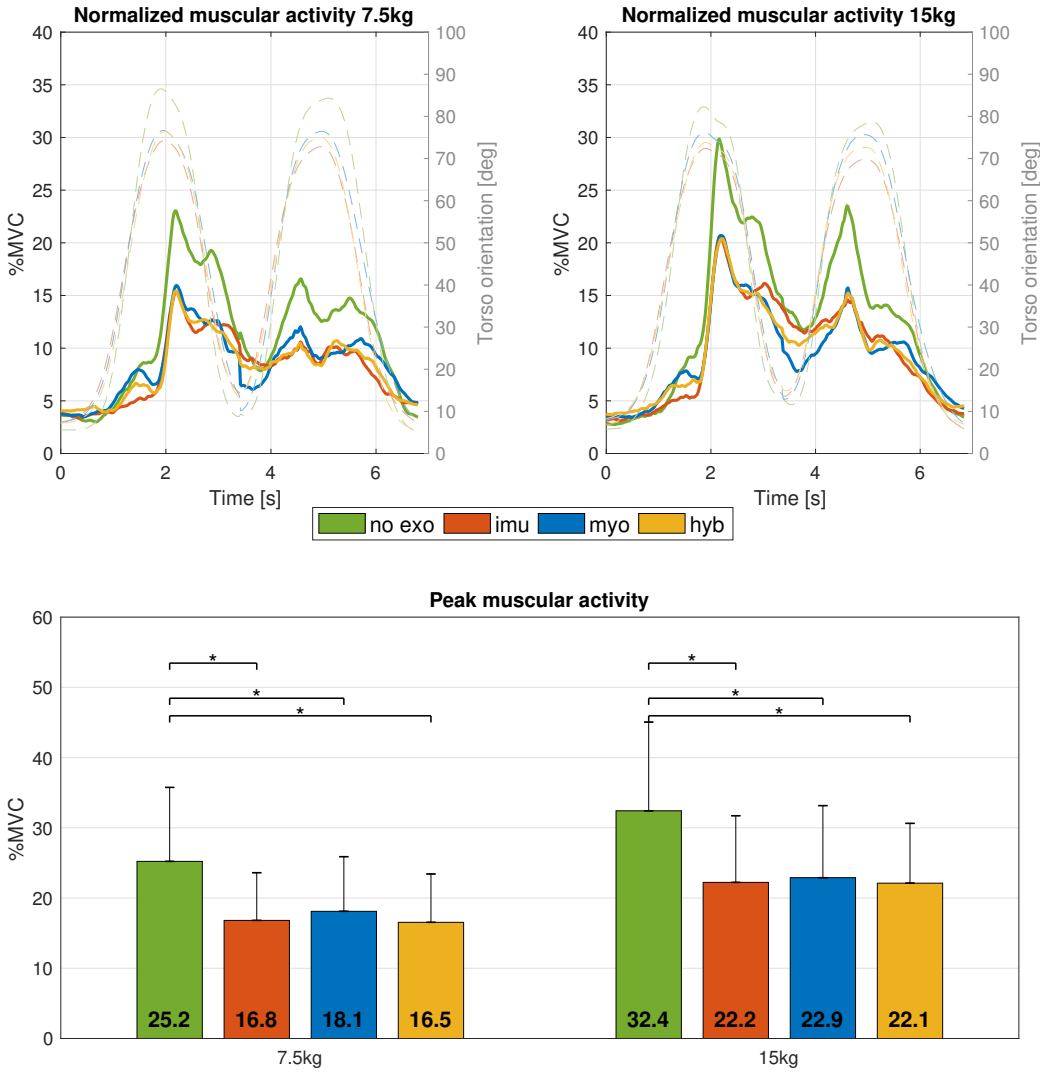

Figure 5.2: Reduction in muscular activity for the different conditions. At the top, averaged EMG profiles across all subjects are shown. In all cases, wearing the exoskeleton is associated to decreased muscular activity, although none of the three strategies leads to overall larger reduction than the others. In terms of peak activity, the data is summarized at the bottom, where average peaks across all subjects are shown for the different conditions. Significant percentage reductions ($p < 0.05$) for the three strategies range between 28% and 35%.

of the specific prototype and encourages further research work aimed at more accurate understanding of the physical effects. As the development of active devices advances, they are expected to achieve even greater reductions in joint loading than passive ones. This is mostly thanks to more appropriate assistive behaviors capable of capturing the conditions that require strongest assistance, e.g. via electromyography (Chapter 4).

Based on the data presented, none of the three appears to prevail over the others in terms of greatest reduction in peak muscular activation, although the difference in timing among them. Rather, *imu* and *myo* display different basic behaviors.Also, as discussed in Section 4.3, *myo* may be scaled up more intuitively than *imu* due to its dependence on the load.

A number of factors limit the direct translation of the results from validation studies in the laboratory into actual use in the field. Certainly, the short duration of the activities during the tests does not fully represent the long hours of operation that workers need to sustain daily. In this respect, physical discomfort may occur in long-term use. Validation studies in the laboratory also typically involve a small number of participants, whereas observations on a larger population would be more adequate for generalization. Additionally, the simplified, symmetric lifting tasks performed in the laboratory may not reflect the real scenarios, where operators may also twist their torso, adopt different lifting techniques based on the shape of loads, and walk between stations. All these extra elements may play a role in both the physical effect of the exoskeleton and how comfortable it is to wear for hours at a time.

In other words, biomechanics testing in the laboratory is a helpful tool to establish starting evidence as well as to build confidence in the devices being developed. However, their validation must be followed with ex-

tended campaigns outside the laboratory, as close as possible to the real scenarios of operation and therefore including the same workers for whom such devices would enter daily use. Besides the device's physical effectiveness, individual preferences are another important aspect that should be considered to promote the use of exoskeletons. In this direction, it may be valuable to provide each user the ability to affect and adjust the control parameters (within certain safety limits) to promote one's own comfort. as it is active and controlled via computers, the device presented would easily implement this possibility.

It should be noted that the torque profiles shown in this chapter are reference values, as opposed to actual torques applied on the user's body. In fact, the low-level performance of the actuators as torque generators as well as of the torque transmission from the actuators to the user's body are areas for future research work, aimed at a more accurate understanding of the physical effect of the exoskeleton on its wearer (as opposed to only measuring muscle activation). In addition, the device used in this study is still a research prototype. Although it has been used in preliminary pilot trials in industrial settings (outside the scope of the present study), it should be taken as a non-final prototype, whose effect may further improve following refinements in its implementation. For example, in the current version the electrical power for the actuators is delivered via a cable by an external supply, which limits the usability of the device to confined, uncluttered spaces where electrical power is available. Battery power for improved mobility and autonomy is part of the plans for future technical development.

6 Conclusion

There has been increasing interest in employing wearable exoskeletons to improve the ergonomics and thus reduce the risk of musculoskeletal injuries in the workplace. Driven by preliminary evidence of their physical benefits, their use is increasingly shifting from the laboratory into the application field, often as collaboration between developers and end users. The potential of *active* exoskeletons in terms of physical benefits is considered to be even greater than that of passive systems [4]. However, the adoption of active exoskeletons appears to be lagging behind by a few years, held back by a number of technical challenges, which are interesting from a research perspective.

This thesis explores technical solutions with the goal of advancing the technical development of active back-support exoskeletons, and thus their readiness for real-life applications. The research work focuses on some aspects of active exoskeletons that are considered particularly impactful to promote their effectiveness and user acceptance, namely actuators and control strategies.

6.1 Contributions

Starting from a critical study of the state of the art (Sections 2.1 and 2.2), this thesis elaborates the overall concept for a new prototype of back-support exoskeleton (Section 2.3). The core contributions of this doctoral research lie in two areas as summarized below.

Actuation

Parallel-elastic actuators (PEAs) represent a valuable solution for the design of dynamic and lightweight active joints for exoskeletons. PEAs make better use of the motor operating range compared to rigid actuators on joints characterized by largely asymmetric loads (Sections 3.1.1 and 3.2). A simplified actuator model (Section 3.3) and relative performance measures are presented to suggest that, thanks the parallel spring, a more convenient choice for the motor can be made. This leads to improved dynamic performance as captured by the proposed measures (Section 3.4), which are associated to user comfort and are thus considered to promote acceptance in the workplace.

Control strategy

The potential advantage of active exoskeletons is dependent on appropriate control strategies. Indeed, their versatility lies in the ability to switch between strategies and adapt to users and task conditions. The central tradeoff in the design of strategies is between the invasiveness of the associated physical sensors and their information content. Two strategies with relevance to different conditions are shown. An indirect strategy that modulates the assistance based on user posture is implemented. It only re-

quires the sensors embedded in the exoskeleton and can support against gravity on the upper body. However, it cannot adjust to external load (Section 4.2.1). To address this shortcoming, a direct strategy based on *proportional myocontrol* is implemented (Section 4.2.2). In contrast with cumbersome laboratory setups for electromyography, this implementation uses a convenient and unobtrusive armband. This solution requires minimal calibration and familiarization, which increases its potential applicability in the field.

6.2 Impact

The present work contributes to the field of active exoskeletons by proposing and supporting solutions for improved effectiveness and user acceptance of these devices. The work is particularly relevant to back-support exoskeletons, which promise to reduce the risk of musculoskeletal back problems for manual workers. The impacts of reduced workplace injuries will include improved quality of life for workers as well as decreased related costs for employers. It is important to stress that the impact will only be tangible if exoskeletons are actually adopted as solutions in the workplace. For this to happen, their technical development still needs to reach a level of advancement whereby workers agree to receive them as part of their standard equipment for certain tasks, and at the same time companies are encouraged to purchase them by affordable costs and effective integration with existing processes.

During the course of the Robo-Mate project (see Section 1.3), one of the industrial partners took the initiative towards the commercial exploitation of the results on the active back-support exoskeleton. A newly-founded

company[1] has been working on the commercialization of the prototype. In the perspective of advancing active exoskeletons and their use in the workplace, this is a small but important success and I personally look forward to witnessing the future progress of this market sector.

6.3 Future work

The research carried out during the three years has addressed a number of open questions, but at the same time many new interesting questions have emerged. Some of the opportunities and goals for further work are discussed below.

- Improved understanding of the dynamics of torque and speed at human joints could lead to more detailed descriptions of dynamic torque requirements for exoskeleton actuators, so that their design can be optimized for specific applications.
- Improved understanding of how to best transfer substantial forces to human limbs via the physical interfaces could improve the level of comfort in using devices. It could also possibly lead to the ability to design and employ stronger actuators, thus further reducing physical loads compared to the current generation.
- The identification of specific physical subtasks of manual handling and corresponding strategy would allow to maximize the beneficial effect of the exoskeleton in multiple activities.

[1] https://www.germanbionic.com/

- Testing campaigns outside the laboratory and in scenarios closer to industrial applications would allow to evaluate the current implementation and inform future improvements in the design.
- Further refinement of the current prototype could improve the physical effectiveness as well as the user acceptance of the existing design.
- Extending the concepts of actuation and/or control interfaces to additional joints (e.g. shoulder, elbow, knee) may provide further support to workers during heavy physical activities.

A PUBLICATIONS

Design

Toxiri, S., Ortiz, J., Masood, J., Fernández, J., Mateos, L. A., & Caldwell, D. G. (2015, December). A wearable device for reducing spinal loads during lifting tasks: Biomechanics and design concepts. In *Robotics and Biomimetics (ROBIO), 2015 IEEE International Conference on* (pp. 2295-2300). IEEE.

Toxiri, S., Ortiz, J., Masood, J., Fernández, J., Mateos, L. A., & Caldwell, D. G. (2017). A powered low-back exoskeleton for industrial handling: considerations on controls. In *Wearable Robotics: Challenges and Trends* (pp. 287-291). Springer International Publishing.

Actuation

Toxiri, S., Calanca, A., Ortiz, J., Fiorini, P., & Caldwell, D. G. (2017). A parallel-elastic actuator for a torque-controlled back-support exoskeleton. *IEEE Robotics and Automation Letters*, 3(1), 492-499.

Control strategy

Toxiri, S., Ortiz, J., & Caldwell, D. G. (2017, June). Assistive Strategies for a Back Support Exoskeleton: Experimental Evaluation. In *International Conference on Robotics in Alpe-Adria Danube Region* (pp. 805-812). Springer, Cham.

Toxiri, S., Koopman, A. S., Lazzaroni, M., Ortiz, J., Power, V., de Looze, M. P., O'Sullivan, L., & Caldwell, D. G. Rationale, Implementation and Evaluation of Assistive Strategies for an Active Back-Support Exoskeleton. SUBMITTED to *Frontiers in Robotics and AI*.

Others

Huysamen, K., de Looze, M., Bosch, T., **Toxiri, S.**, Ortiz, J., & O'Sullivan, L., (2018). Assessment of an active industrial exoskeleton to aid dynamics lifting and lowering manual handling tasks. *Applied Ergonomics, 68*, 125-131.

Stadler, K., Altenburger, R., Schmidhauser, E., Scherly, D., Ortiz, J., **Toxiri, S.**, & Masood, J. (2017). ROBO-MATE: AN EXOSKELETON FOR INDUSTRIAL USE - CONCEPT AND MECHANICAL DESIGN. In *Advances in Cooperative Robotics* (pp. 806-813).

Mateos, L. A., Ortiz, J., **Toxiri, S.**, Fernández, J., Masood, J., & Caldwell, D. G. (2016, June). Exoshoe: a sensory system to measure foot pressure in industrial exoskeleton. In *Biomedical Robotics and Biomechatronics (BioRob), 2016 6th IEEE International Conference on* (pp. 99-105). IEEE.

Masood, J., Mateos, L. A., Ortiz, J., **Toxiri, S.**, O'Sullivan, L., & Caldwell, D. G. (2017). Active Safety Functions for Industrial Lower Body Exoskeletons: Concept and Assessment. In *Wearable Robotics: Challenges and Trends* (pp. 299-303). Springer International Publishing.

BIBLIOGRAPHY

[1] G. Colombo, M. Joerg, R. Schreier, and V. Dietz, "Treadmill training of paraplegic patients using a robotic orthosis," *Journal of rehabilitation research and development*, vol. 37, no. 6, p. 693, 2000.

[2] H. Kawamoto, S. L. S. Lee, S. Kanbe, and Y. Sankai, "Power assist method for HAL-3 using EMG-based feedback controller," in *IEEE International Conference on Systems, Man and Cybernetics*, vol. 2, 2003, pp. 1648–1653.

[3] A. B. Zoss, H. Kazerooni, and A. Chu, "Biomechanical Design of the Berkeley Lower Extremity Exoskeleton (BLEEX)," *IEEE/ASME Transactions on Mechatronics*, vol. 11, no. 2, pp. 128–138, 2006.

[4] M. P. de Looze, T. Bosch, F. Krause, K. S. Stadler, and L. W. O'Sullivan, "Exoskeletons for industrial application and their potential effects on physical work load," *Ergonomics*, vol. 0139, no. December, pp. 1–11, 2015.

[5] OHSA (European Agency for Safety and Health at Work), "OSH in figures: Work-related musculoskeletal disorders in the EU - Facts and figures," *Publications Office of the European Union*, 2000.

[6] S. Konz, "NIOSH lifting guidelines," *American Industrial Hygiene Association Journal*, vol. 43, no. 12, pp. 931–933, 1982.

[7] T. R. Waters, V. Putz-anderson, A. Garg, and L. J. Fine, "Revised NIOSH equation for the design and evaluation of manual lifting tasks," *Ergonomics*, vol. 36, no. 7, pp. 749–776, 1993.

[8] A. Garg, "Revised NIOSH equation for manual lifting: a method for job evaluation," *American Association of Occupational Health Nurses Journal*, vol. 43, no. 4, pp. 211–216, 1995.

[9] T. Bosch, J. van Eck, K. Knitel, and M. de Looze, "The effects of a passive exoskeleton on muscle activity, discomfort and endurance time in forward bending work," *Applied Ergonomics*, vol. 54, pp. 212–217, 2016.

[10] N. P. Reeves and J. Cholewicki, "Modeling the human lumbar spine for assessing spinal loads, stability, and risk of injury," *Critical Reviews in Biomedical Engineering*, vol. 31, no. 1&2, 2003.

[11] M. P. De Looze, I. Kingma, W. Thunnissen, M. J. Van Wijk, and H. M. Toussaint, "The evaluation of a practical biomechanical model estimating lumbar moments in occupational activities," *Ergonomics*, vol. 37, no. 9, pp. 1495–1502, 1994.

[12] I. Kingma, M. P. de Looze, H. M. Toussaint, H. G. Klijnsma, and T. B. M. Bruijnen, "Validation of a full body 3-D dynamic linked segment model," *Human Movement Science*, vol. 15, no. 6, pp. 833–860, 1996.

[13] C. K. Anderson, D. B. Chaffin, G. D. Herrin, and L. S. Matthews, "A biomechanical model of the lumbosacral joint during lifting activities," *Journal of Biomechanics*, vol. 18, no. 8, pp. 571–584, 1985.

[14] K. Naruse, S. Kawai, H. Yokoi, and Y. Kakazu, "Development of wearable exoskeleton power assist system for lower back support," in *Intelligent Robots and Systems, 2003.(IROS 2003). Proceedings. 2003 IEEE/RSJ International Conference on*, vol. 4. IEEE, 2003, pp. 3630–3635.

[15] Z. Luo and Y. Yu, "Wearable stooping-assist device in reducing risk of low back disorders during stooped work," in *Mechatronics and Automation (ICMA), 2013 IEEE International Conference on*. IEEE, 2013, pp. 230–236.

[16] M. Abdoli-E, M. J. Agnew, and J. M. Stevenson, "An on-body personal lift augmentation device (PLAD) reduces EMG amplitude of erector spinae during lifting tasks," *Clinical Biomechanics*, vol. 21, pp. 456–465, 2006.

[17] Y. Imamura, T. Tanaka, Y. Suzuki, K. Takizawa, and M. Yamanaka, "Motion-based design of elastic belts for passive assistive device using musculoskeletal model," in *2011 IEEE International Conference on Robotics and Biomimetics, ROBIO 2011*, no. 1, 2011, pp. 1343–1348.

[18] M. Wehner, D. Rempel, and H. Kazerooni, "Lower Extremity Exoskeleton Reduces Back Forces in Lifting," in *ASME 2009 Dynamic Systems and Control Conference, Volume 2*, no. OCTOBER 2009, 2009, pp. 49–56.

[19] B. L. Ulrey and F. A. Fathallah, "Subject-specific, whole-body models of the stooped posture with a personal weight transfer device,"

Journal of Electromyography and Kinesiology, vol. 23, no. 1, pp. 206–215, 2013.

[20] J. Babič, K. Mombaur, D. Lefeber, J. van Dieën, B. Graimann, M. Russold, N. Šarabon, and H. Houdijk, "SPEXOR: Spinal Exoskeletal Robot for Low Back Pain Prevention and Vocational Reintegration," in *Wearable Robotics: Challenges and Trends, Biosystems and Biorobotics*, 2017, vol. 16, pp. 311–315.

[21] L. de Rijcke, M. Näf, B. Graimann, H. Houdijk, J. van Dieën, K. Mombaur, M. Russold, N. Sarabon, J. Babič, and D. Lefeber, "SPEXOR: Towards a Passive Spinal Exoskeleton," in *Wearable Robotics: Challenges and Trends, Biosystems and Biorobotics*, 2017, vol. 16, pp. 325–329. [Online]. Available: http://link.springer.com/10.1007/978-3-319-46532-6

[22] M. B. Naef, L. De Rijcke, C. Rodriguez Guerrero, M. Millard, B. Vanderborght, and D. Lefeber, "Towards Low Back Support with a Passive Biomimetic Exo-Spine," in *International Conference on Rehabilitation Robotics (ICORR)*, 2017, pp. 1165–1170.

[23] T. Aida, H. Nozaki, and H. Kobayashi, "Development of muscle suit and application to factory laborers," in *IEEE International Conference on Mechatronics and Automation, ICMA 2009*, 2009, pp. 1027–1032.

[24] H. Hara and Y. Sankai, "Development of HAL for lumbar support," in *SCIS and ISIS 2010 - Joint 5th International Conference on Soft Computing and Intelligent Systems and 11th International Symposium on Advanced Intelligent Systems*, 2010, pp. 416–421.

[Online]. Available: http://www.scopus.com/inward/record.url?eid=2-s2.0-84866716169{&}partnerID=tZOtx3y1

[25] K. S. Stadler, R. Altenburger, E. Schmidhauser, D. Scherly, J. Ortiz, S. Toxiri, L. Mateos, and J. Masood, "ROBO-MATE AN EXOSKELETON FOR INDUSTRIAL USECONCEPT AND MECHANICAL DESIGN," in *Advances in Cooperative Robotics*. World Scientific, 2017, pp. 806–813.

[26] S. Toxiri, J. Ortiz, J. Masood, J. Fernandez, L. A. Mateos, and D. G. Caldwell, "A Wearable Device for Reducing Spinal Loads during Lifting Tasks: Biomechanics and Design Concepts," in *International Conference on Robotics and Biomimetics*, 2015, pp. 2295–2300.

[27] S. Wang, W. Van Dijk, and H. Van Der Kooij, "Spring uses in exoskeleton actuation design," *IEEE International Conference on Rehabilitation Robotics*, pp. 0–5, 2011.

[28] N. G. Tsagarakis, S. Morfey, H. Dallali, G. A. Medrano-Cerda, and D. G. Caldwell, "An Asymmetric Compliant Antagonistic Joint Design for High Performance Mobility," in *IEEE/RSJ International Conference on Intelligent Robots and Systems (IROS)*, 2013, pp. 5512–5517.

[29] M. Grimmer, M. Eslamy, S. Gliech, and A. Seyfarth, "A comparison of parallel-and series elastic elements in an actuator for mimicking human ankle joint in walking and running," *IEEE International Conference on Robotics and Automation*, pp. 2463–2470, 2012.

[30] R. Jimenez-Fabian, J. Geeroms, L. Flynn, B. Vanderborght, and D. Lefeber, "Reduction of the torque requirements of an active ankle

prosthesis using a parallel spring," *Robotics and Autonomous Systems*, vol. 92, pp. 187–196, 2017.

[31] W. Roozing, Z. Li, G. A. Medrano-Cerda, D. G. Caldwell, and N. G. Tsagarakis, "Development and Control of a Compliant Asymmetric Antagonistic Actuator for Energy Efficient Mobility," *IEEE/ASME Transactions on Mechatronics*, vol. 21, no. 2, pp. 1080–1091, 2016.

[32] T. Verstraten, P. Beckerle, R. Furnémont, G. Mathijssen, B. Vanderborght, and D. Lefeber, "Series and Parallel Elastic Actuation: Impact of natural dynamics on power and energy consumption," *Mechanism and Machine Theory*, vol. 102, pp. 232–246, 2016.

[33] H. Hara and Y. Sankai, "HAL equipped with passive mechanism," in *2012 IEEE/SICE International Symposium on System Integration, SII 2012*, 2012, pp. 1–6.

[34] P. Beckerle, T. Verstraten, G. Mathijssen, R. Furnemont, B. Vanderborght, and D. Lefeber, "Series and Parallel Elastic Actuation: Influence of Operating Positions on Design and Control," *IEEE/ASME Transactions on Mechatronics*, vol. 22, no. 1, pp. 521–529, 2017.

[35] A. Calanca, R. Muradore, and P. Fiorini, "A Review of Algorithms for Compliant Control of Stiff and Fixed-Compliance Robots," *IEEE/ASME Transactions on Mechatronics*, vol. 21, no. 2, pp. 613–624, 2016.

[36] J. Masood, J. Ortiz, J. Fernandez, L. A. Mateos, and D. G. Caldwell, "Mechanical Design and Analysis of Light Weight Hip Joint Parallel Elastic Actuator for Industrial Exoskeleton," in *IEEE RAS/EMBS*

International Conference on Biomedical Robotics and Biomechatronics (BioRob), 2016, pp. 631–636.

[37] D. E. Whitney, "Force Feedback Control of Manipulator Fine Motions," *Transactions of the ASME Journal of Dynamical Systems Measurement Control*, vol. 99, no. 2, pp. 91–97, 1977.

[38] B. Ugurlu, M. Nishimura, K. Hyodo, M. Kawanishi, and T. Narikiyo, "Proof of Concept for Robot-Aided Upper Limb Rehabilitation Using Disturbance Observers," *IEEE Transactions on Human-Machine Systems*, vol. 45, no. 1, pp. 110–118, 2015.

[39] J. S. Sulzer, R. A. Roiz, M. A. Peshkin, and J. L. Patton, "A Highly Backdrivable , Lightweight Knee Actuator for Investigating Gait in Stroke," *IEEE Transactions on Robotics*, vol. 25, no. 3, pp. 539–548, 2009.

[40] D. Zanotto, T. Lenzi, P. Stegall, and S. K. Agrawal, "Improving transparency of powered exoskeletons using force/torque sensors on the supporting cuffs," in *IEEE International Conference on Rehabilitation Robotics*, 2013, pp. 0–5.

[41] M. Eslamy, M. Grimmer, and A. Seyfarth, "Effects of Unidirectional Parallel Springs on Required Peak Power and Energy in Powered Prosthetic Ankles: Comparison between Different Active Actuation Concepts," in *International Conference on Robotics and Biomimetics, IEEE*, 2012, pp. 2406–2412.

[42] S. Toxiri, J. Ortiz, J. Masood, J. Fernandez, L. A. Mateos, and D. G. Caldwell, "A powered low-back exoskeleton for industrial handling: considerations on controls," in *Internation Symposium on Wearable Robotics*, 2016.

[43] J. Lobo-prat, P. N. Kooren, A. H. A. Stienen, J. L. Herder, B. F. J. M. Koopman, and P. H. Veltink, "Non-invasive control interfaces for intention detection in active movement-assistive devices," *Journal of NeuroEngineering and Rehabilitation*, vol. 11, no. 1, pp. 1–22, 2014.

[44] A. J. Young and D. P. Ferris, "State-of-the-art and Future Directions for Robotic Lower Limb Exoskeletons," no. August, 2016.

[45] A. Ansari, C. G. Atkeson, H. Choset, and M. Travers, "Estimating Operator Intent (Draft 4.0)," Tech. Rep., 2015. [Online]. Available: http://www.cs.cmu.edu/{~}cga/exo/intent.pdf

[46] M. R. Tucker, J. Olivier, A. Pagel, H. Bleuler, M. Bouri, O. Lambercy, J. d. R. Millán, R. Riener, H. Vallery, and R. Gassert, "Control strategies for active lower extremity prosthetics and orthotics: a review," *Journal of NeuroEngineering and Rehabilitation*, vol. 1, no. 12, 2015.

[47] T. Yan, M. Cempini, C. Maria, and N. Vitiello, "Review of assistive strategies in powered lower-limb orthoses and exoskeletons," *Robotics and Autonomous Systems*, vol. 64, pp. 120–136, 2015.

[48] B. Chen, H. Ma, L.-y. Qin, F. Gao, K.-m. Chan, S.-w. Law, L. Qin, and W.-h. Liao, "Recent developments and challenges of lower extremity exoskeletons," *Journal of Orthopaedic Translation*, vol. 5, pp. 26–37, 2016.

[49] A. Ahmed, H. Cheng, X. Lin, M. Omer, and J. Atieno, "Survey of On-line Control Strategies of Human-Powered Augmentation Exoskeleton Systems," *Advances in Robotics & Automation*, vol. 05, no. 03, 2016.

[50] R. Ronsse, T. Lenzi, N. Vitiello, B. Koopman, E. Van Asseldonk, S. M. M. De Rossi, J. Van Den Kieboom, H. Van Der Kooij, M. C. Carrozza, and A. J. Ijspeert, "Oscillator-based assistance of cyclical movements: Model-based and model-free approaches," *Medical and Biological Engineering and Computing*, vol. 49, no. 10, pp. 1173–1185, 2011.

[51] F. Giovacchini, F. Vannetti, M. Fantozzi, M. Cempini, M. Cortese, A. Parri, T. Yan, D. Lefeber, and N. Vitiello, "A light-weight active orthosis for hip movement assistance," *Robotics and Autonomous Systems*, vol. 73, pp. 123–134, 2015.

[52] V. Ruiz Garate, A. Parri, T. Yan, M. Munih, R. M. Lova, N. Vitiello, and R. Ronsse, "Experimental validation of motor primitive-based control for leg exoskeletons during continuous multi-locomotion tasks," *Frontiers in Neurorobotics*, vol. 11, no. MAR, 2017.

[53] J. E. Pratt, B. T. Krupp, C. J. Morse, and S. H. Collins, "The RoboKnee: An Exoskeleton for Enhancing Strength and Endurance During Walking," in *IEEE International Conference on Robotics and Automation*, 2004.

[54] Y. Ikeuchi, J. Ashihara, Y. Hiki, H. Kudoh, and T. Noda, "Walking Assist Device with Bodyweight Support System," in *IEEE/RSJ International Conference on Intelligent Robots and Systems*, 2009, pp. 4073–4079.

[55] L. Saccares, A. Brygo, I. Sarakoglou, and N. G. Tsagarakis, "A Novel Human Effort Estimation Method for Knee Assistive Exoskeletons," in *International Conference on Rehabilitation Robotics (ICORR)*, 2017, pp. 1266–1272.

[56] W. Kim, J. Lee, L. Peternel, N. Tsagarakis, and A. Ajoudani, "Anticipatory Robot Assistance for the Prevention of Human Static Joint Overloading in Human Robot Collaboration," *IEEE Robotics and Automation Letters*, vol. 3, no. 1, pp. 68–75, 2018.

[57] H. Kazerooni, J.-l. Racine, L. Huang, and R. Steger, "On the Control of the Berkeley Lower Extremity Exoskeleton (BLEEX)," in *Proceedings of the 2005 IEEE International Conference on Robotics and Automation*, no. April, 2005, pp. 4364–4371.

[58] M. Wehner, "Man to Machine, Applications in Electromyography," *EMG Methods for Evaluating Muscle and Nerve Function*, p. 29, 2012.

[59] M. Hakonen, H. Piitulainen, and A. Visala, "Current state of digital signal processing in myoelectric interfaces and related applications," *Biomedical Signal Processing and Control*, vol. 18, pp. 334–359, 2015.

[60] J. Rosen, M. Brand, M. B. Fuchs, and M. Arcan, "A Myosignal-Based Powered Exoskeleton System," *IEEE Transactions on Systems, Man, and Cybernetics*, vol. 31, no. 3, pp. 210–222, 2001.

[61] T. Hayashi, H. Kawamoto, and Y. Sankai, "Control Method of Robot Suit HAL working as Operator' s Muscle using Biological and Dynamical Information," in *IEEE/RSJ International Conference on Intelligent Robots and Systems*, 2005.

[62] C. Fleischer and G. Hommel, "A Human-Exoskeleton Interface Utilizing Electromyography," *IEEE Transactions on Robotics*, vol. 24, no. 4, pp. 872–882, 2008.

[63] N. Karavas, A. Ajoudani, N. Tsagarakis, J. Saglia, A. Bicchi, and D. Caldwell, "Tele-Impedance based Stiffness and Motion Augmentation for a Knee Exoskeleton Device," in *IEEE International Conference on Robotics and Automation*, 2013.

[64] T. Lenzi, S. M. M. De Rossi, N. Vitiello, and M. C. Carrozza, "Intention-based EMG control for powered exoskeletons," *IEEE Transactions on Biomedical Engineering*, vol. 59, no. 8, pp. 2180–2190, 2012.

[65] L. Grazi, S. Crea, A. Parri, T. Yan, M. Cortese, F. Giovacchini, M. Cempini, G. Pasquini, S. Micera, and N. Vitiello, "Gastrocnemius myoelectric control of a robotic hip exoskeleton," in *Proceedings of the Annual International Conference of the IEEE Engineering in Medicine and Biology Society, EMBS*, vol. 2015-Novem, 2015, pp. 3881–3884.

[66] A. J. Young, H. Gannon, D. P. Ferris, and A. J. Young, "A Biomechanical Comparison of Proportional Electromyography Control to Biological Torque Control Using a Powered Hip Exoskeleton," *Frontiers in Bioengineering and Biotechnology*, vol. 5, no. June, 2017.

[67] R. Meattini, G. Palli, and C. Melchiorri, "Experimental Evaluation of a sEMG-Based Control for Elbow Wearable Assistive Devices During Load Lifting Tasks," in *International Conference on Rehabilitation Robotics (ICORR)*, 2017, pp. 140–145.

[68] J. Lobo-Prat, P. N. Kooren, A. H. Stienen, J. L. Herder, B. F. Koopman, and P. H. Veltink, "Non-invasive control interfaces for intention detection in active movement-assistive devices," *Journal of NeuroEngineering and Rehabilitation*, vol. 11, no. 1, p. 168, 2014.

[69] W. S. Kim, H. D. Lee, D. H. Lim, J. S. Han, K. S. Shin, and C. S. Han, "Development of a muscle circumference sensor to estimate torque of the human elbow joint," *Sensors & Actuators A: Physical*, vol. 208, pp. 95–103, 2014.

[70] A. Parri, K. Yuan, D. Marconi, T. Yan, S. Crea, M. Munih, R. M. Lova, N. Vitiello, and Q. Wang, "Real-time Hybrid Locomotion Mode Recognition for Lower-limb Wearable Robots," *IEEE/ASME Transactions on Mechatronics*, vol. PP, no. 99, p. 1, 2017.

[71] H. J. Hermens, B. Freriks, R. Merletti, D. Stegeman, J. Blok, G. Rau, C. Disselhorst-Klug, and G. Hägg, "European recommendations for surface electromyography," *Roessingh research and development*, vol. 8, no. 2, pp. 13–54, 1999.